Fast DC Charging Infrastructures for Electric Vehicles: Overview of Technologies, Standards, and Challenges

Pasquale Franzese, *Student Member, IEEE*, Dhruvi Dhairya Patel, *Student Member, IEEE*, Ahmed A. S. Mohamed, *Senior Member, IEEE*, Diego Iannuzzi, *Member, IEEE*, Babak Fahimi, *Fellow, IEEE*, Massimo Risso, and John M. Miller, *Life Fellow, IEEE*

***Abstract*— This article is an overview of fast charging for electrical vehicles. Specifically, it analyzes the impact of ultrafast charging stations (UFCSs) on the distribution grid and their role in the smart grids. Moreover, this article defines the framework of UFC, its diffusion, and the associated new trends. The most frequently used converters in the conversion stages of dc charging stations with integrated generation are analyzed. To achieve this goal four active front-end ac–dc converters (unidirectional and bidirectional), three isolated dc–dc converters and two control architectures are explored. In comparing the targeted configurations, the main target is set on categorizing them based on supply voltage level, type of smart grid, and power flow of the converters. Furthermore, this article outlines a broad overview of the main standards for UFCSs and the evaluation of the reliability, data collection, and operation of UFCSs. This article aims to link the needs of the designers of charging stations to the preferences of the commercial market.**

***Index Terms*— AC–DC converter, data usage, dc charge, dc–dc converter, electric vehicle supply equipment (EVSE), reliability assessment, smart grid, ultrafast charging station (UFCS).**

Acronyms and Nomenclature

AFE	Active front end.
BESS	Battery energy storage system.
BMS	Battery management system.
CAN	Control area network.
CCC	Controlled current charge.
CCS	Combined charging system.
CERTS	Consortium for electric reliability technology solutions.
CHB	Cascaded H-bridge.
CP	Control pilot.
CPO	Charge point operator.
CVC	Controlled voltage charge.
DAB	Dual active bridge.
DBC	Dead beat control.
DER	Distributed energy resource.
DG	Distributed generation.
DME	DER managing entity.
DSO	Distribution system operator.
EES	Electrical energy storage.
EMF	Electromagnetic field.
EMSP	E-mobility service provider.
EPS	Electric power system.
EV	Electric vehicle.
EVSE	EV supply equipment.
FMEA	Failure mode and effect analysis.
G2V	Grid to vehicle.
HFT	High-frequency transformer.
MMC	Modular multilevel converter.
MPC	Model predictive control.
LFT	Line-frequency transformer.
MCS	Megawatt charging system.
MRAC	Model reference adaptative control.
NPC	Neutral-point-clamped.
PCC	Point of common connection.
PEV	Plug-in EV.
PF, PFC	Power factor correction.
PHEV	Plug-in hybrid EV.
PLC	Power line communication.
PoD	Point of delivery.
PV	Photovoltaic panels.
RBS	Reliability block scheme.
RCA	Root cause analysis.
RES	Renewable energy source.
SGAM	Smart grid architecture model.
SGIC	Grid information clearinghouse.
SoC	State of charge.
SoH	State of health.
SST	Solid-state transformer.
SVM	Space-vector modulation.
UFC	Ultrafast charging.

Manuscript received 23 June 2022; revised 21 October 2022; accepted 9 January 2023. Date of publication 23 January 2023; date of current version 13 September 2023. *(Corresponding author: Diego Iannuzzi.)*

Pasquale Franzese and Diego Iannuzzi are with the Department of Electrical Engineering and Information Technology (DIETI), University of Napoli – Federico II, 80125 Naples, Italy (e-mail: pasquale.franzese@unina.it; diego.iannuzzi@unina.it).

Dhruvi Dhairya Patel and Babak Fahimi are with the Department of Renewable Energy and Vehicular Technology Laboratory (REVT), University of Texas at Dallas, Richardson, TX 75080 USA (e-mail: Dhruvi.Patel2@utdallas.edu; fahimi@utdallas.edu).

Ahmed A. S. Mohamed is with National Renewable Energy Laboratory, Golden, CO 80401 USA (e-mail: ahmed.mohamed@nrel.gov).

Massimo Risso is with Nidec ASI s.p.a., 20092 Cinisello Balsamo (MI), Italy (e-mail: massimo.risso@nidec-asi.co).

John M. Miller is with the Power Electronics and Electric Power Systems Research Center, Oak Ridge National Laboratory (ORNL), Oak Ridge, TN 37830 USA (e-mail: jmmiller35@aol.com).

Digital Object Identifier 10.1109/TTE.2023.3239224

2332-7782 © 2023 IEEE. Personal use is permitted, but republication/redistribution requires IEEE permission.
See https://www.ieee.org/publications/rights/index.html for more information.

Authorized licensed use limited to: Universita degli Studi di Napoli Federico II. Downloaded on January 09,2025 at 10:42:23 UTC from IEEE Xplore. Restrictions apply.

UFCS	UFC station.
V2G	Vehicle to grid.
VCCF	Vehicle charge control function.
WT	Wind turbine.

I. Introduction

COMMERCIALIZATION of electrified vehicles has rapidly grown over the recent years and is attracting the interest of not only car makers but also their entire suppliers. By the end of 2020, there was an increment in the number of EVs on the roads reaching ten million units globally [1].

Even though the markets suffered from the pandemic, the sales of EVs managed to grow by 41% in 2020, despite global car sales dropping by about 16%. In the first quarter of 2021, global electric car sales have been around 140% more than those in the same period in 2020. China leads with 500k vehicles sold followed closely by Europe with 450k, while in the U.S., the sales were doubled compared to the first quarter of 2020 [1].

In 2016, the European Union (EU) proposed a low-emission mobility strategy to simplify the travel by EVs making EV charging as easy as filling a conventional vehicle [2]. The U.S., instead, provided a tax credit for the purchase of a new qualified PEV, which includes a battery storage system with a minimum capacity of 5 kWh that uses an external energy source to recharge the battery while meeting specified emission standards.

The EV market is affected by consumer perception of cost/return of investment, public incentives, technological advances, government policies, city planning, and power utility impact on the diffusion of EV charging infrastructure. The distribution, location, and types of EVSE depend on the urbanization of the area, the EV target, and travel patterns. The number of private chargers installed in 2020 amounts to 9.5 million, while seven million were installed at residential sites, and the remaining stations are at public places [1]. Moreover, a recent analysis has shown that the use of public chargers will almost completely take over home charging, and people without access to home charging will start buying EVs [3].

Strategic roadmaps for electromobility and integrated policies on vehicles and charging infrastructures are mainly coordinated at the regional level, and most countries do not have national development plans in place yet. For a successful market take-up of PEV, UFCSs along the highway network are a necessity [4]. In Europe, more than 38k public fast chargers are being installed, up 55% in 2020, including nearly 4k in France, 2k in The Netherlands, 6.2k in the U.K., and 7.5k in Germany [5]. According to the Alternative Fuels Infrastructure Directive (AFID) recommendation, the ratio between the PEVs and charging points must be lower than 10 in each EU Member State [6].

During the years leading to the development of EVs and EVSEs, the terms slow, fast, quick, super, ultra, and so on were used to describe charging capabilities.

Notably, the charging power level that can be considered high for a motorcycle could be viewed as low for a truck. Moreover, a 40-min charge is considered more feasible than a charging time of several hours during the night. However, it is slower than the 20-min charging time required by modern vehicles. For these reasons, one can use the definition according to the standards.

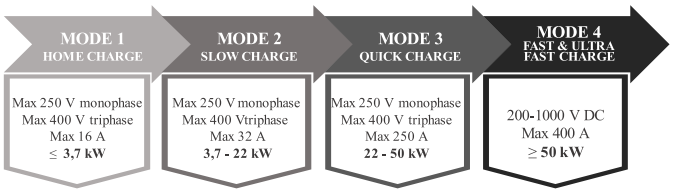

Fig. 1. Standard charging modes by Tu et al. [124].

This article offers an overview of UFCSs as an emerging component of smart grids to highlight the most critical topics in the assignment of requirements according to the existing standards, type of grid connection, and choice of converter topology. Moreover, additional aspects, such as reliability, communication, and data usage, are explored.

This article comprises six sections. Section I deals with the footprint of UFCSs on the distribution network and the interrelation between the smart grids, DG, and the UFCSs. Section II presents a comparison among the various electrical topologies based on the connection with the grid, the connection of the subsystem within the microgrid, and the most frequently used ac–dc and dc–dc converters. In Section III, a guideline on the standards defined for smart grids, renewable sources, storage systems, and UFCSs (power requirement communication and protocols) is provided. Sections IV and V include an evaluation of the reliability and data collection and usage of a UFCS. The article includes a list of the newest electrical vehicles that accept UFC.

II. UFCSs as Part of Smart Grids

A review of the state-of-the-art for UFCSs starts with the definition of a UFCS, and the context and the network in which they are installed. In this section, the connection between UFCSs, smart microgrids, and DG is analyzed. This includes the influence that integration has on the electrical topology of charging stations.

A. What Is the UFC?

The international standard [124] defines four charging modes, as shown in Fig. 1. The charging mode referred to as UFC is Mode 4. Mode 4 comprises a dc charger with a power range exceeding 50 kW; all the charging powers that are higher than 50 kW are treated by the same set of regulations in terms of electrical topologies of converters, communication protocols, connectors, safety, and reliability. More details on the charging classification are described in Section III.

Nowadays, a charging power of 50 kW is not enough to be considered ultrafast, especially for large trucks. The trend used by manufacturers and owners of chargers is to consider a provided power higher than 120 kW as ultrafast, but this value could change over time.

The new trend of required power and energy implies a change in the design and sizing of batteries, not only in terms of capacity but also in terms of voltage level. Given an equal capacity and charging power, a battery storage system with

Authorized licensed use limited to: Universita degli Studi di Napoli Federico II. Downloaded on January 09,2025 at 10:42:23 UTC from IEEE Xplore. Restrictions apply.

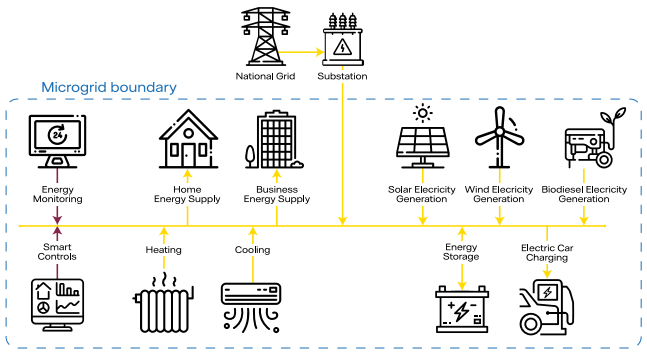

Fig. 2. Example scheme of a smart microgrid.

a low-voltage level needs higher current, so higher losses on cables and converters, bigger conductors and terminals, higher cooling, and a typically more complex BMS to balance the cells. The battery storage system with a higher voltage level needs lower current, but that brings isolation issues and more constraints on the choice of converters topologies (i.e., if the supplier has a voltage lower than that of the battery, the conversion stage must be an active step-up converter). These observations are resulting in an increase in the voltage level of the batteries used in large or heavy vehicles. To get an idea of voltage levels, today, most of the small or medium cars may have a range of voltage up to 400 V, while large or heavy vehicles have a nominal voltage of around 800 V.

B. Historical Perspective on Smart Grids

In the U.S., the Energy Independence and Security Act gave the first official definition of smart grid in 2007 with regard to the modernization of energy transmission and distribution services. This was followed by the American Recovery and Reinvestment Act of 2009, which mandates measures to modernize the nation's infrastructure. Specifically, the Department of Energy (DoE) is charged with coordinating grid modernization to become a "smart" grid. The DoE Office of Electricity Delivery and Energy Reliability heads this effort with the National Institute of Standards and Technology (NIST) coordinating the development of standard models and protocols for information management to achieve interoperability of smart grid systems and devices.

According to [7], the term "smart grid" refers to a digitized electric grid and enables to manage power and energy according to the conditions of producers and consumers by including more advanced communication, control, and sensory technology. An example is shown in Fig. 2.

C. Footprint of the UFCSs on the Distribution Network

A smart microgrid is an effective form for the integration of DG into the network; it must be able to measure, predict, and manage the flow of power between sources and loads. The UFCS, basically, is an energy-greedy load for a microgrid, which, if not managed correctly, can cause distribution grid issues. The international report [7] describes the provisional EV chargers' energy and power demand until 2030; the results are reported in Fig. 3. The substantial rise in the required

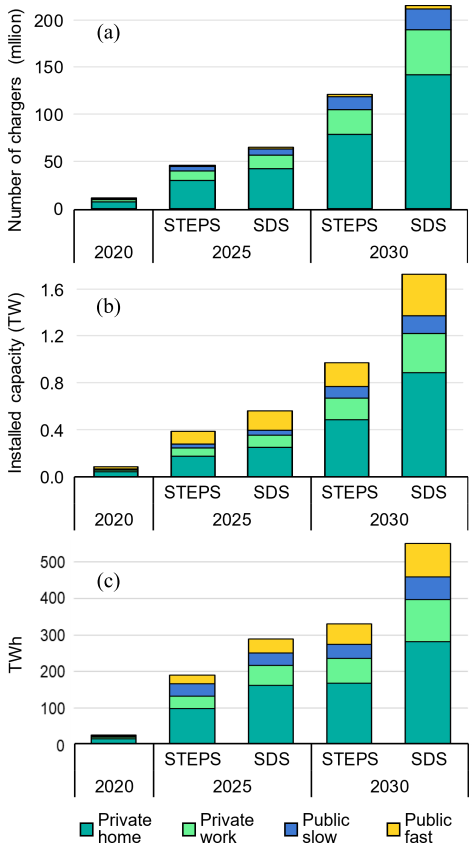

Fig. 3. (a) Electric LDV chargers. (b) Demand for installed charging power. (c) Demand for charging energy by scenario 2020–2030 by the international report [7].

installed power offers an outlook on the growing impact of EV chargers on the electric network.

Depending on the location of the chargers and the charging times, the EVs present extra electrical loads having an impact on the distribution grid in terms of voltage deviations and power losses. From both the DSO's and the customers' points of view, the transformer and supplier overloads must be avoided, and the power losses during charging must be minimized. Uncoordinated charging of EVs may lead not only to power losses but also to power quality issues, frequency instability, harmonics injection, and voltage collapse, to name a few.

In [8], the impacts of a residential feeder of 10 kV on the distribution grid are analyzed in terms of voltage quality, power loss, load profile, and several penetration level scenarios. The smart charging method sets the chargeable power dynamically and adapts to the dispatching operation requirements flexibly, and the impacts on the grid can be reduced. Furthermore, the large, multiutility collaborative study in [9] provides an analytical model to evaluate the impact of PHEV loading on DSO's operations.

In [10] and [11], the potential impacts of charging operations are analyzed with emphasis on peak demand and load profile, voltage variations and distortions, voltage imbalance (for single-phase operation), and violation of legal limits. Moreover, Alam et al. [12] propose an extensive approach to evaluate the adverse impact of different levels of EV penetration on the loss of useful lifetime in distribution transformers.

Authorized licensed use limited to: Universita degli Studi di Napoli Federico II. Downloaded on January 09,2025 at 10:42:23 UTC from IEEE Xplore. Restrictions apply.

The proposed method is applied to a sample distribution transformer supplying residential customers. This strategy is able to vary the peak-shaving support depending on the level of the stored energy in the PEV battery. The proposed strategy varies the peak load support based on the trend of the load profile. In [8], the impact of the charging of the EVs on the distribution network and a resolution with an optimal design of a smart grid have been analyzed.

D. Smart Grid and DGs

The design of smart charging stations can improve the coordination of power flow among the grid, the EVSEs, and the EVs [13], fulfilling the significant increase in EVs' power demand.

Recent studies have shown that the bidirectional power flow in distribution networks, induced by the significant deployment of DG, can affect the voltage levels and the quality of the power supply. This topic is also dealt with in [14] within the specific context of the U.S.

The DG makes the current faults, the phase imbalance, and the network protection system faults easier to be detected and managed. In this context, proper coordination of charging and discharging of EVs also plays a role in handling many ancillary services and continuously forcing the grid into stable regions.

A detailed overview of energy storage and renewables is presented in [15]. In [16], several topologies of electrochemical, mechanical, chemical, thermal, electrical, and hybrid ESSs for microgrid and EV applications are presented and compared. The selection criteria and economic evaluation of the integration of an ESS are explored in [17]. The standard [18] establishes requirements and criteria for the interconnection of DERs with EPSs.

Among DGs, the V2G mode of slow charging EVSE, presented as prototypes only, begins to be an exploitable reality. If there is a large number of slow bidirectional chargers integrated into a microgrid, they can help the grid or microgrid to supply the UFCSs.

In [19], smart charging strategies to implement G2V and V2G in a unified framework are proposed for the optimal integration of PEVs within the existing distribution grid.

In [20], the proposed decentralized V2G control methods contribute to primary frequency control; in addition, a centralized supplementary frequency regulation (SFR) of interconnected power systems with many EVs is studied. Simulation results show that the fluctuation of area control error (ACE) and system frequency can be effectively suppressed. By balancing between regulation-up and regulation-down tasks, battery energy at expected SOC levels can be achieved. In [21], an off-line strategy is implemented to determine the duration of V2G service and the desired level of peak shaving. The strategy is based on the real-time dynamic adjustment of the PEV mobility model and the estimated loading profile. It is shown that 8% PEV V2G penetration corresponds to a peak shaving rate of approximately 99% on a 1-MVA-rated transformer. In [22], a smart charging station that is placed near a distribution node area and can perform V2G has been introduced. In [23] and [24], an urban distribution system is modeled and simulated to demonstrate V2G capabilities, such as meeting voltage drop reduction and peak demand. The simulations are conducted using the fuzzy logic controller (FLC). In [13], the functionality and feasibility of the regulation of a grid ancillary service through the EV's battery are evaluated. These publications illustrate the new opportunities in using EV chargers/ultrafast chargers for improvement of the regulation and stability of the microgrid and distribution grid. This is in direct contrast with the initial view on chargers as being difficult and problematic loads in modern microgrids and smart grids.

E. EV Chargers With Integrated Generation

The most frequently used function performed by a smart microgrid is the equalization of the power flow via of peak shaving [12], [21], [25], [26], [27], [28], [29], [30], load shifting [31], [32], [33], [34], [35], [36], [37], and load leveling [38], [39], [40].

These techniques of equalization alongside devices that generate and store energy can be used in the smart control of EVSEs.

Global leveling refers to the direct interface of the station to the entire distribution grid. Using this approach, the grid becomes the single supplier for the EV charger. In [8], a coordinated network of charging structures is proposed to maximize the main grid load factor and minimize power losses. In this article, deterministic household profiles together with uncoordinated and coordinated charging of the PHEV batteries are discussed, assuming an accurate knowledge of the forecast consumption. In [41], the EV chargers are inserted into a smart grid in which the operating costs and investment of conventional generation assets with a flexible demand are optimized through a novel planning model. Case studies in the U.K. demonstrate that EV flexibility significantly flattens the net demand by reducing peak demand levels and absorbing the variability introduced by wind generation, and subsequently impacts the optimal generation mix by allowing the cost-effective integration of a larger proportion of base load generation. In [42], several controlled charging schemes are compared in order to control energy prices and to indirectly influence charging operations. The performance targets, such as ensuring fairness, maximizing the operator's profit, and minimizing power loss, are achieved by controlling a wide set of charging parameters in smart charging patterns. In [43], a scheduling method for EV chargers is proposed to minimize the operational costs under the technical constraints required by transmission and DSOs. The results show that, in the presence of smart charging, the EV aggregator can benefit from additional degrees of freedom compared to two cases of uncoordinated charging while adhering to technical constraints. The savings are at least 5% and become significant when EV penetration levels increase. This is because total EV uncoordinated charging tends to overpass technical operator constraints. In [44], the impact of uncoordinated, coordinated, and smart EV charging on a microgrid under security constraints is investigated.

Authorized licensed use limited to: Universita degli Studi di Napoli Federico II. Downloaded on January 09,2025 at 10:42:23 UTC from IEEE Xplore. Restrictions apply.

Global leveling is not a sufficiently acceptable solution for UFC because, although the stations connected to the MV grid can be supplied directly with the required power, the same is not true for stations that are connected to the LV grid. Therefore, adding DGs and ESSs as proper parts of the station becomes inevitable. In this case, the local leveling entails the management of these smart microgrids that are integrated into charging stations.

There are several different ways to arrange and control a system consisting of renewable DG, energy storage, EV chargers, and the electric grid. This poses an open research question in which architecture and control methodology can provide the most practical solution from the cost and performance points of view. The solution to this question comes with a quantitative comparison of the alternative architectures in terms of cost, efficiency, and reliability. In [10], a comparison of alternative designs for an architecture equipped with storage, integrated renewable DG, and grid-interfaced PEV chargers, based on financial asset costs and operating costs (consisting of maintenance and energy costs), is presented. The introduced costs help to study the impact of system reliability and efficiency on the results. Moreover, in [10], a conceptual methodology to optimize the design and sizing is applied to a system with a single storage unit, a single renewable distributed generator, and a single charger. Notably, the presented framework is also applicable to systems with multiple storage units, sources, and chargers. In summary, the abovementioned publications emphasize the additional degrees of freedom, rendered by smart management of EV chargers and EV ultrafast chargers, in better coordination of power flow, peak shaving, and accessibility to power within a microgrid. This, in turn, provides higher efficiency at a lower cost of production and distribution of power.

F. Charging Station With Multiple Plug-In Slots

A multiple-slot station is different from multiple single-slot stations; the main difference is the use of shared resources.

The number of components that allows the station to interface with the vehicles depends on the number of vehicles; thus, it is the same for both solutions. Having n single-slot stations, it means multiplying all the components to connect the station to the grid by n, thus increasing the costs. For this reason, a multiple-slot station is a more flexible and cheaper solution.

In slow charging, the solution of a multiple-slot station also offers the possibility of a simpler V2G implementation.

The multiple-slot station has an extra standard constraint, which is related to the explicit galvanic isolation of each slot from the others. This constraint is already satisfied by the single-slot stations because isolation from the grid also allows for isolation among the charging slots.

The multiple-slot stations need management of energy flows, queuing, and shared resources, such as the ESS. Among the features offered by multiple-slot stations, three are given in the following.

1) *Power Sharing (Load Balancing):* The maximum available power is equally distributed across all active dispensers and the other loads.
2) *Power Boost (Peak Shaving):* The supplied power is that required by each charger and by the rest of the loads. When the power is reaching its maximum value, the supplied power is proportionally reduced by the smart charging control system.
3) *Dynamic Power Sharing:* It is a combination of power boost and power sharing. When the demand by other loads is lower than the maximum capacity, the extra available power is automatically distributed among other chargers. Otherwise, if the demand by other loads is equal to or greater than the maximum available value, no power is supplied to the charging stations.

The matters of queuing and management of shared resources are very broad, and interested readers can refer to [45].

III. Electrical Structures of UFCSs

In this section, UFCSs are classified according to the magnitude of their operating voltage criteria. The type of grid connection (LV or MV) determines the voltage and power, hence the size of the converters and their performance. The electrical topology of the station depends on the approach used to connect the conversion subsystems together. The approach may be through an ac, a dc, or a hybrid microgrid.

Various concepts of electric infrastructure for UFCSs are presented in the following to link each topology with its features and the requirements that it helps to meet.

A. LV or MV Supply Network

While the standards on the interface between charging stations and EVs are international, the guidelines on voltage and current values of the interface between the station and network are inherently dependent on the aspects of the network; these characteristics are not globally identical.

As per the international standard [46], the definitions of LV and MV for both ac and dc electricity supply systems are not well established. The grid sizes of our interest are called band 1 and band 2, and they have a range of voltage from 100 V to 1 kV for LV and from 1 kV to 35 kV for the subdistribution level, respectively. In addition, [47] subdivides connection points into four distinct classes, based on the size and voltage; Type B has an installed power between 11.08 kW and 6 MW. Every country outlines the details on voltage and frequency levels and the classification of the networks in HV, MV, and LV. In this article, the LV grid is considered to have a magnitude of 400 V in a three-phase voltage connection and a power of less than 100 kW; the MV grid has voltage and power levels higher than 1 kV and 100 kW.

In an MV supply network, it is mandatory to have a connection to the grid via MV PoD. The typical required steps are given as follows.

1) Request for a power increase to the energy provider.
2) Installation of the MV cabinet, the MV/LV transformer, including the entire set of instrumentation, equipment of the local energy distributor, and other civil works. Often, the MV cabinet is already installed, and this step is not required.
3) Installation of the new LV PoD, MV and LV cables, and civil works to connect the main electric panels, and

Authorized licensed use limited to: Universita degli Studi di Napoli Federico II. Downloaded on January 09,2025 at 10:42:23 UTC from IEEE Xplore. Restrictions apply.

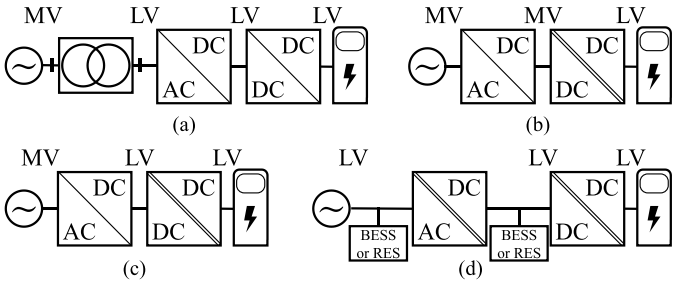

Fig. 4. Topologies of grid connection of UFCSs. (a) MV network with an MV/LV LFT, LV ac–dc, and LV dc–dc. (b) MV network with an MV/MV ac–dc and MV/LV dc–dc. (c) MV network with an MV/LV ac–dc and LV dc–dc. (d) LV network with BESSs and/or RESs.

modification of the MV main electric panel to feed the new UFCS.

4) Checking and confirmation by the energy provider and the appropriate authority.

On the other hand, the installation of an infrastructure that is directly connected to the LV grid needs only a request for a power increase to the energy provider (the power is limited within the LV range) and the modification of the already existing LV PoD, if necessary.

Even though the costs may change depending on the country, the MV connection has definitely higher initial and maintenance costs than the LV connection. The LV-coupled infrastructures are also typically easier for integration with renewable sources of energy.

The classification of charging stations based on network interface is explained in the following and is shown in Fig. 4.

1) MV Network With an MV/LV LFT, LV AC–DC, and LV DC–DC: Fig. 4(a) describes a simplified block diagram of a low-voltage dc fast-charging system architecture. The UFCS is fed from the MV distribution grid, an LFT that converts MV to LV, and an LV ac–dc rectification stage is followed by the dc–dc power conversion stage, which is interfaced with the vehicle battery.

The use of a heavy and large service transformer for the ac distribution bus introduces significant installation costs, bulky LV distribution switchgear equipment, and large conductors [48]. Thus, this type of UFCS architecture may not be suitable for limited spaces or in the absence of an MV/LV substation, which may occur in urban or metropolitan areas.

2) MV Network With an MV/MV AC–DC and MV/LV DC–DC: The recently published research pushes toward new solutions with the charging stations that are directly connected to the MV distribution grid without heavy and bulky service transformers [see Fig. 4(b)].

In the literature, this architecture looks like the most widespread type in UFCS applications. The rectifier unit converts MVAC to MVDC and maintains the bias bus voltage, while a dc–dc converter supplies the vehicle at the LV value. Typically, the latter is composed of a modular multilevel structure in which the conversion blocks are installed in input-series output-parallel [49].

Moreover, compared to the solution with the SST, LV ac–dc, and LV dc–dc, this proposed architecture only requires a single-stage PFC/rectification unit, thereby reducing the overall conversion stages.

An example of this topology is given in [50]. This system presents a fast-charging station composed of a central ac–dc bidirectional converter of MMC type, able to provide ancillary services. The charging station in [51] is composed of an ac–dc CHB converter followed by a set of modular DAB dc–dc current-fed converters. The CHB converter is controlled to balance the dc voltage for both charging and discharging modes. Nair and Fernandes [52] propose a dc fast-charging station that can charge EV batteries with different power and voltage levels thanks to the control of a power electronic architecture. In [53], the main conversion stage of the proposed charging system has identical ac–dc power modules on each phase of the three-phase ac input. The outputs of the power modules are connected in parallel to the dispenser. The converter uses a combination of double-phase shift (DPS) and single-phase shift (SPS), and a variable switching frequency to achieve high-power quality and a wide ZVS range.

3) MV Network With an MV/LV AC–DC and LV DC–DC: An alternative topology is illustrated in Fig. 4(c), where the MV/LV conversion is in the dc–dc converter, and the ac–dc converter also reduces the voltage level from MV to LV.

In [54], [55], and [56], an SST is used instead of a conventional LFT to convert the MV into LV and to provide galvanic isolation. In [54] and [57], a brief classification of the SST topology is proposed.

The EV charging station in [58] is implemented with an MV DAB converter with 3.3−kV SiC MOSFETs. In [59], the investigators at North Carolina State University propose an EV charging solution at 350 kW, which block MV input voltage of 12.47 kV using $10-$ kV SiC MOSFETs.

4) LV Network With BESSs and/or RESs: The LV-interfaced infrastructures have lower costs of installation and maintenance even though the price of kWh may be higher than that of an MV grid. The cost and volume of an MV cabinet and its safety requirements discourage the diffusion of the MV connection in busy urban areas or remote suburbs.

The maximum value of power available through the LV connection is less than the required target power of the UFC. The storage and renewable sources are sized to boost the power and balance the power supplied by the grid and that required by the load. The ac–dc and dc–dc converters are all in LV, and the DGs might be interfaced on both ac and dc connection points [see Fig. 4(d)].

Mahfouz and Iravani [60] present, develop, and evaluate a charging station equipped with battery energy storage, which can decouple the dynamics of the grid from those of the station, operating in islanded or grid-connected mode. Franzese and Iannuzzi [61] deal with mathematical modeling and the control system for UFCS based on the dc microgrid and BESS. The sizing of the BESS and the overall energy supervisory control are discussed. In [62], the prototype of UFCS realized at the University of Naples Federico II is highlighted. The LV-connected charger is discussed in terms of configuration and rated values.

B. AC, DC, and Hybrid Microgrids

1) AC Microgrid: In a microgrid built as an ac-coupled architecture, the RESs, BESSs, and the EV chargers are connected to the common ac bus, as shown in Fig. 5(a); the PV

Authorized licensed use limited to: Universita degli Studi di Napoli Federico II. Downloaded on January 09,2025 at 10:42:23 UTC from IEEE Xplore. Restrictions apply.

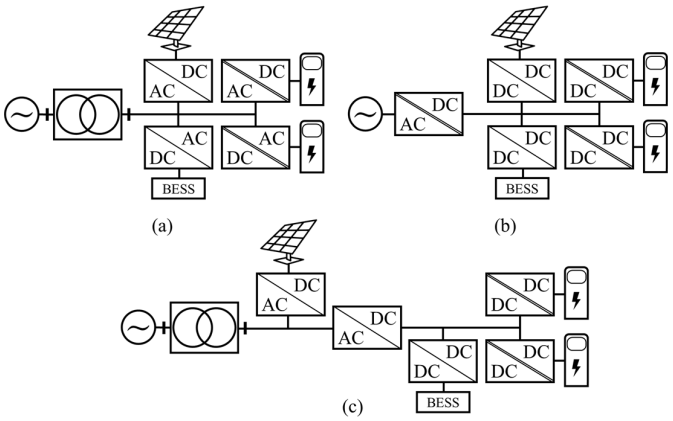

Fig. 5. Scheme of UFCS as (a) ac, (b) dc, and (c) hybrid microgrids.

panels, the BESS, and the dispenser of the EVs are connected using dedicated ac–dc converters, while the WTs, the utility grid, and other types of ESS are connected using ac/ac converters or with LFTs. Due to its well-defined standards and the availability of ac products in the market [63], [64], [65], [66], [67], [68], [69], the ac-coupled architecture is a good choice for home chargers.

The advantage of this architecture is that the decoupling controls of both active and reactive power may assure stable voltage, and the voltage can be easily stepped up or down using transformers. Moreover, the components may be sized independently, and they can be also distributed over a long distance. Since the dc loads are the dominant type in the UFCS, there is the disadvantage that, for each source or load, an ac–dc conversion stage is required; this penalizes the efficiency.

Liu et al. [65] introduce a study on the ac microgrid, including power generation units, PV, WT, controllable/uncontrollable loads, and smart EV chargers. Tabrizi et al. [66] use an EV charger station based on an ac microgrid to evaluate the improvement of the grid frequency and voltage profile through the use of renewable energy.

2) DC Microgrid: The dc-coupled microgrid architecture is shown in Fig. 5(b). It consists of BESS, a PV system with MPPT, power converters, EV chargers, and a central controller.

The presence of the common dc bus allows for easier and more efficient use of the PV system, and in general, less power loss and high-power transmission capacity are provided by the absence of reactive power [70], [71]. In [72] and [73], the central control consists of two control loops: the dc bus voltage direct control and the current control, which manages the power flow. In this way, the energy exchanged among the different energy sources and loads is efficiently coordinated.

In [74], the feasibility of different operating modes is evaluated on the dc-based charging system integrating renewable sources. In [75], the dc-based microgrid, equipped with PV panels, is designed to meet the changing needs. A strategy to control the microgrid under different load conditions and dc voltage levels is also proposed.

It is important to note that, in a multislot charging station, standards impose galvanic insulation among the chargers and between the chargers and the grid. In an ac microgrid, the insulation is provided through SSTs or LFTs, even if the latter is bulkier. The dc–dc converters used in dc microgrids are isolated through HFTs; the main advantage is the lower volume of converters for the same power conversion.

3) AC–DC Hybrid Microgrid: The electrical topology, able to provide the advantages of both ac-based and dc-based smart microgrids, is the hybrid ac–dc structures, as shown in Fig. 5(c). Generally, the hybrid microgrid is considered an ac grid with the dc grid as a particular dc load/source.

In the ac–dc hybrid microgrid, the fundamental equipment for connecting the ac and dc sides is the interlinked power converter (ILC). According to the actual needs of the grid, the ILC can work in the rectifier or inverter mode [76], [77], [78]. It allows the power exchange between the ac and dc sides while maintaining the energy balance.

Jia et al. [77], Aryani et al. [77], and Amirkhan et al. [79] propose an investigation into the influence of EVs on hybrid microgrids, including storage systems. Unamuno and Barrena [80] provide a review and classification of different hybrid ac–dc microgrid topologies. In [81] and [76], the connection between the three-phase ac side and dc side is analyzed to evaluate the impacts of heterogeneous and homogeneous EV loads under balanced and unbalanced scenarios. A three-layer concerted control system is implemented into the central microgrid controller. In [82], an EV charging station based on a hybrid CERTS microgrid is implemented, and the performance characteristics are evaluated.

A comparison of ac, dc, and hybrid microgrids is given in Table I.

In practical applications, a big part of dc charger producers employs the topology shown in Fig. 4(a) with or without the dc–dc converter and the microgrid shown in Fig. 5(b). This is because most refueling stations on the highways are already equipped with an MV/LV substation and a certified transformer. Typically, the diffusion of an electrical topology, rather than others, does not follow the design evaluation by the manufacturers of the charger. This is typically based on the requirements of the charging point operators (CPOs) and the charging station owners.

With reference to the power architectures of the power converter systems between dc MGs, ac grids, and hybrid dc-MGs, other classifications into three categories can be considered. This includes single, parallel, and aggregated converter systems. The single converter to link the dc MG and the ac grid is usually used in small-scale systems. In [83], a PV-wind-battery hybrid MG has been considered as a model reference to represent the ac and dc hybrid MGs. In [84], an integrated configuration is used with one ac–dc–ac back-to-back converter as the power hub to connect both ac and dc grids. In particular, the ac MG and ac utility grid are connected to the two ac sides of the ac–dc–ac converters, respectively. Meanwhile, the dc link of the converter is connected to the dc MG. In order to increase the exchanged power capability, parallel interface converters can be employed between the ac and dc bus. In [85], parallel bidirectional interlinking inverters are used to connect the dc grids and ac grids.

In addition, the hybrid dc-MGs can be also classified in terms of the topologies of dc MG, i.e., single-bus topology, multibus topology, and reconfigurable topology, respectively [83]. At a lower power level, a possible classification is based on dc-bus technology. This includes direct battery

Authorized licensed use limited to: Universita degli Studi di Napoli Federico II. Downloaded on January 09,2025 at 10:42:23 UTC from IEEE Xplore. Restrictions apply.

TABLE I
COMPARISON OF AC, DC, AND HYBRID MICROGRIDS

AC MICROGRID	**Advantages** – Well-developed standards and more available technologies. – Decentralized interface with grid and single control of active/reactive power. – Easy expansion over long distances. **Disadvantages** – The cost of multiple AC-DC converters with low-power is higher than that of a single high-power converter. – Multiple AC-DC converters can produce undesirable harmonic distortions on the power grid.
DC MICROGRID	**Advantages** – High flexibility of the structure; it can quickly integrate RES and ESS. – High-power transmission capacity and high efficiency. – Less volume in DC-DC converters. **Disadvantages** – More expensive and complex protection devices required because no zero cross points of the voltage exist.
HYBRID MICROGRID	**Advantages** – Elimination of redundant multiple conversion processes and reduction of total conversion losses. – Elimination of dedicated rectifiers for AC and DC loads, that means cost reduction and simplification of electronic equipment. **Disadvantages** – No specific protocols to evaluate the feasibility and scope of the hierarchical and master-slave control of the microgrid in the integrated system.

connection, single unipolar regulated bus, bipolar regulated bus, multiple regulated buses structure, single-side transformer (SST)-enabled MG, dc ring bus, zonal dc MG, and MTDC MG [72].

C. Comparison of Converter Topologies

1) AC–DC Converters in UFCSs: Regardless of the type of grid connection and the type of common bus, the conversion stages are composed of ac–dc and dc–dc converters. In order to help with the selection of the microgrid topology, an overview of the most commonly used converters for UFCSs is presented.

The ac–dc converters provide an interface between the grid or the ac part of the microgrid, as well as a dc bus. The main requirements for these converters are to regulate the output voltage, shape the input current, and ensure high power quality on both ac and dc sides [86], [87]. Typically, in UFCS applications without additional sources and storage, only unidirectional power flow is required from ac–dc converters.

1) The simplest topology is the passive diode bridge, as illustrated in Fig. 6(a). Both the single- and three-phase converters are widely used and are available on the market. This converter does not need control drivers, and the cost is very low. Its output dc voltage is fixed in polarity and magnitude, which is lower than the input phase-to-phase voltage.

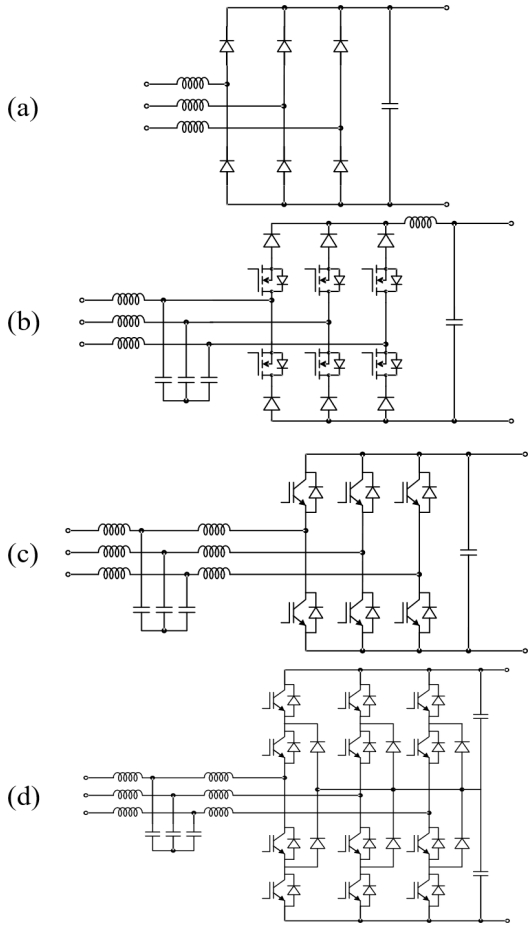

Fig. 6. AC–DC converters for UFCSs. (a) Passive diode bridge. (b) Buck-type unidirectional PWM converter. (c) Active front end. (d) NPC converter.

If the variation of the output voltage is an important feature, a buck-type unidirectional ac–dc converter, as shown in Fig. 6(b), can be used. The lower output voltage and the simple inrush current control are the main advantages of this converter (the same is true for other boost-type topologies). In this converter, the higher the phase shift between the input current and voltage, the lower is the output voltage reference. This topology has generally higher conduction losses but lower switching losses [88]. The classical current controls of this converter are very similar to those of the three-phase active PWM converter. A well-structured overview of this converter and its control is given in [89].

1) The most widely used ac–dc converter in UFCSs is the three-phase PWM converter, also called AFE, with an LCL filter. This configuration is shown in Fig. 6(c). The bidirectional flow of power makes this converter ideal for hybrid microgrids, which means connecting sources and loads to ac or dc side. This converter generates low-harmonic input currents and enables arbitrary power factor regulation. In [90], two AFE converters for recharging infrastructure applications are presented; both LF and HF isolation requirements are discussed.

Authorized licensed use limited to: Universita degli Studi di Napoli Federico II. Downloaded on January 09,2025 at 10:42:23 UTC from IEEE Xplore. Restrictions apply.

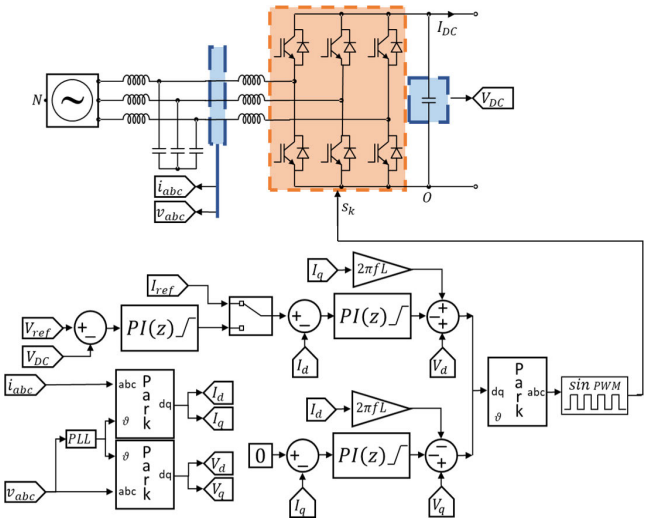

Fig. 7. AFE control scheme: CV or CC control.

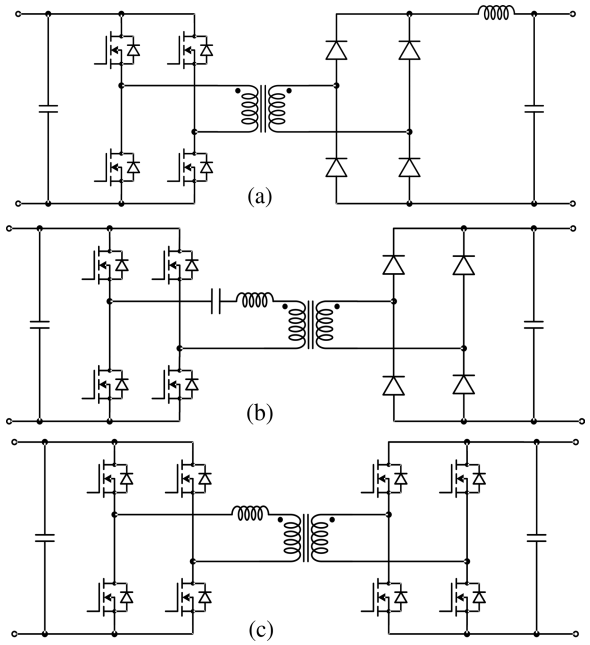

Fig. 8. Electrical topologies of the most used dc–dc converters in dc charging stations. (a) SAB converter. (b) LLC converter. (c) DAB converter.

It must be noted that the objective, in this configuration, is to control the ac voltage and the dc-bus voltage at the required reference value. A classical control scheme based on the SVM technique is implemented using PI controllers to regulate the current on the d-axis and the q-axis. The block diagram of this control is shown in Fig. 7; the values V_{ref} and I_{ref} are used to implement controlled voltage and controlled current modes.

A substantial number of the SVM controls are proposed in the literature even though only a select few have been actually utilized in practice. DBC, finite control set MPC, and modulated MPC are examples proposed in [91], [92], and [93]. In [89], sectional-optimized SVM and switching pattern arrangements are proposed. In [94], the design of a simplified predictive control of the dynamics of the dc-link reference voltage in an AFE rectifier is presented. The control does not require additional external control loops, and it does not exhibit an overshoot due to the dynamic reference derived from the mathematical model. An effective MRAC on the AFE converter is proposed in [95]. Zhang et al. [96] deal with a multiple-vector direct model predictive power control (MV-DMPPC). Control using a sliding-mode observer (SMO) is proposed in [97] to estimate the external load which is connected (online) to the dc-link of the AFE and to control the voltage loop that mitigates the fluctuation.

1) The NPC converter, as shown in Fig. 6(d), is another common bidirectional boost-type converter. The main advantages compared to the AFE are the lower voltage ratings for the devices. These results in lower switching losses, even if there are more devices. In [98], the EV charger prototype, with an NPC front end, provides 30 kW at low THD in the input current, filtered by the leakage inductance of the input transformer. Celanovic and Boroyevich [99] explore the properties and the limitations of the balancing problem of the neutral-point voltage of an NPC for different loading conditions. Rivera et al. [100] report on the implementation of an EV charger with a bipolar dc bus using an NPC. Yacoubi et al. [101] study the performance of a three-phase three-level NPC boost rectifier controlling the PF, and the neutral point and output voltages with three control techniques: linear, nonlinear, and nonlinear MRACs. In [102], a new MPC scheme is studied for NPC single-phase three-level PWM rectifiers. In [103], a constant switching frequency model-based adaptive direct power control (MB-ADPC) for three-phase three-level NPC converters is proposed.

The other proposed structures in the literature are more complex, even if they may be more efficient or have reduced volume and costs. For example, in [104], the entire conversion stage is composed of a six-legged inverter with three ports (for the grid, a charging slot, and an ESS) and a high-frequency link transformer as an interface. In [105], an integrated isolated SST with high frequency for fast EV chargers is proposed. In that article, the input current low-order harmonics elimination through the ac–dc conversion stage of the SST is identified and evaluated over a wide range of output dc voltages. In [57], a seven-level grid-tied CHB converter-based fast-charging station is developed.

2) DC–DC Converters in UFCSs: A dc–dc converter always follows the ac–dc front end to interface the RES, ESS, and EV slots to the dc-link. In EV applications, this type of converter needs galvanic isolation to decouple and protect the grid and the charging slots. If the station is a single slot, the isolation with the grid is enough to meet the safety standards. However, if the station has more than one slot, isolated dc–dc converters are mandatory to decouple the charging slots from each other. A comprehensive review of the isolated dc–dc converters is provided in [106] and [107].

If only unidirectional power flow is required, such as in most cases, a potential implementation is the single active bridge (SAB) converter, as also reported in Fig. 8(a). This converter operates under ZVS during turn-on if phase-shifted PWM control is implemented; however, it suffers from turn-off losses in the active switches and high losses in the output diodes. Furthermore, the resonance of the LCL filter, composed of the transformer leakage inductance, the output inductor, and

Authorized licensed use limited to: Universita degli Studi di Napoli Federico II. Downloaded on January 09,2025 at 10:42:23 UTC from IEEE Xplore. Restrictions apply.

the parasitic capacitance of the reverse-biased diodes, leads to a potentially large ringing. Modulation strategies used for inverters can be used on the H-bridge on the primary side. Typically, the HF transformer in this converter handles square waves. This is because no specifications on THD and power factor are required. The block diagram of this control is shown in Fig. 9; the values V_{ref} and I_{ref} are used to denote controlled voltage and controlled current modes.

1) The LLC resonant converter, as shown in Fig. 8(b), is a unidirectional isolated dc–dc converter applied for UFC in the literature. The switching frequency is changed to control output voltage, which is adjusting the impedance of the equivalent resonant load. In the LLC converter, the reduction of turn-off losses and transformer losses are obtained ensuring ZVS with the regulation of the magnetizing current [108]. In [109], the LLC converter of an EV charger may always operate in the resonant frequency range with maximum efficiency because the input voltage is regulated by an ac–dc converter. Although this method is simple and effective, and it does not require extra hardware, it is not suitable for a wide output-voltage range. In [110], the state plane analysis enables to design a frequency control strategy for an LLC resonant dc–dc converter. The proposed control technique in [111] allows tracking the variable resonant frequency for a parallel boost LLC dc–dc converter.
2) The DAB converter, as shown in Fig. 8(c), can be used when a bidirectional power flow is required. It has high efficiency, high-power density, low device stress, buck and boost capability, low sensitivity to component variation, and small filter components. Recently, the advances in the amorphous and nanocrystalline soft magnetic materials and the capabilities of the new GaN- and SiC-based power semiconductor devices have been attracting attention to the DAB converter [112]. The DAB converter is becoming a new prevalent choice in power conversion due to its power density and efficiency.

In the DAB converter, the power flow is controlled by regulating the phase shift between the primary and secondary voltages using the transformer leakage inductance. The available types of phase shift control are SPS, DPS, triple-phase shift (TPS), and extended phase shift (EPS). This converter has been frequently mentioned in the recent literature, and a significant number of comparisons between control strategies have been carried out [113], [114], [115], [116], [117], [118], [119].

However, other nonisolated dc–dc converter topologies can be considered for the new UFCS. An interesting proposal for dc–dc converters used in fast charging applications is the interleaved multichannel buck–boost converter, which increases power density and efficiency [90], [120], [121]. In this case, the isolated stage was made at the level of the first stage of the ac–dc rectifier with a transformer. Another more promising solution is the partial power processing (PPP) dc–dc converter [122]. The power converter is based on the PPP concept, which processes only a small percentage of the total power going from the source to the load. This leads to an improvement in the overall efficiency of the system but negatively affects the PPP architectures, which can never guarantee galvanic isolation. Furthermore, in recent years,

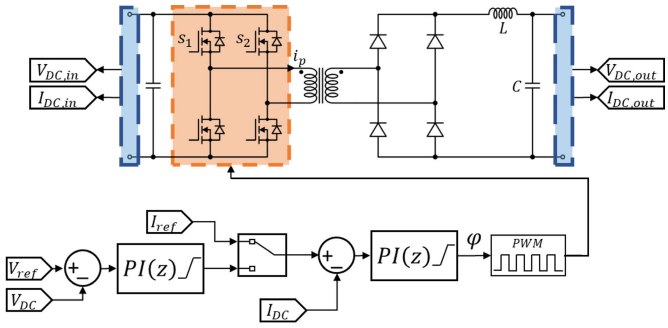

Fig. 9. SAB control scheme: CV or CC control.

the legislation on charging stations for EVs is undergoing significant changes. For example, the requirement of galvanic isolation is under discussion, and in some cases, the application of nonisolated power supply equipment for charging EVs is allowed [123]. To be more precise, the only countries that fall under the rectification of the legislation are the United States of America and Canada. Although there are only two countries that allow nonisolated solutions, they can be considered prominent examples that can encourage others to follow the same path.

In Table II, a matching of the topologies of grid connection with the proposed converters is presented; it may be used as a guideline to select a conversion chain. The marked cells represent suggestions of electrical topologies for ac–dc and dc–dc converters in each topology of Fig. 4. For example, in both conversion chains with one of the two converters working in MV on one side [see Fig. 4(b) and (c)], the boost converters are discouraged. In the topology equipped with the BESS and/or RES, the choice of ac–dc depends on the additional sources that are used. In the presence of a battery on the dc common bus, the dc bus should be at a higher voltage than that of ac side and dispenser side because the battery works better if it is sized with many cells in series.

In Fig. 10, the performance benchmarking of proposed converters is presented using radar diagrams. They are collected from several references, in particular, [124] and [125]. The right reading of that figure is considering less area as higher performance; this is because the positive features, such as bidirectionality, power factor range, and ZVS, are considered with their complements, but the negative features, such as the number of components, THD, losses, and control complexity, are simply normalized. For example, the NPC converter has the highest score for the number of components because it is the converter that needs the highest number of components, increasing the costs. The DAB converter has the minimum score of bidirectionality, which means that it has the highest performance in bidirectionality because it is the only bidirectional presented converter.

Fig. 10 does not provide a final comparison of converters because lots of performances depend on the working conditions, and the right choice of conversion stages depends on many factors.

IV. Standards in UFC: Existing and New

The need for standardization in UFCS, as for any other technical area, is driven by the need for safety, interoperability, coexistence, and performance. Safety covers products and

Authorized licensed use limited to: Universita degli Studi di Napoli Federico II. Downloaded on January 09,2025 at 10:42:23 UTC from IEEE Xplore. Restrictions apply.

TABLE II
MATCHING TABLE OF TOPOLOGIES OF GRID CONNECTION (SEE FIG. 4) WITH PROPOSED AC–DC AND DC–DC CONVERTERS (SEE FIGS. 6 AND 8)

	Passive diode bridge (Fig. 6a)	Buck-type unidirectional PWM converter (Fig. 6b)	Active Front End (Fig. 6c)	NPC converter (Fig. 6d)	
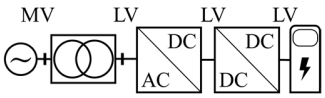	X	X			Single Active Bridge (SAB) converter (Fig. 8a)
	X				LLC converter (Fig. 8b)
	X				Dual Active Bridge (DAB) converter (Fig. 8c)
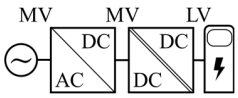	X	X			Single Active Bridge (SAB) converter (Fig. 8a)
					LLC converter (Fig. 8b)
					Dual Active Bridge (DAB) converter (Fig. 8c)
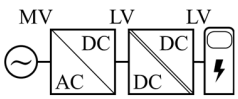	X	X			Single Active Bridge (SAB) converter (Fig. 8a)
					LLC converter (Fig. 8b)
					Dual Active Bridge (DAB) converter (Fig. 8c)
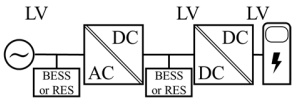			X	X	Single Active Bridge (SAB) converter (Fig. 8a)
	X	X	X	X	LLC converter (Fig. 8b)
	X	X	X	X	Dual Active Bridge (DAB) converter (Fig. 8c)

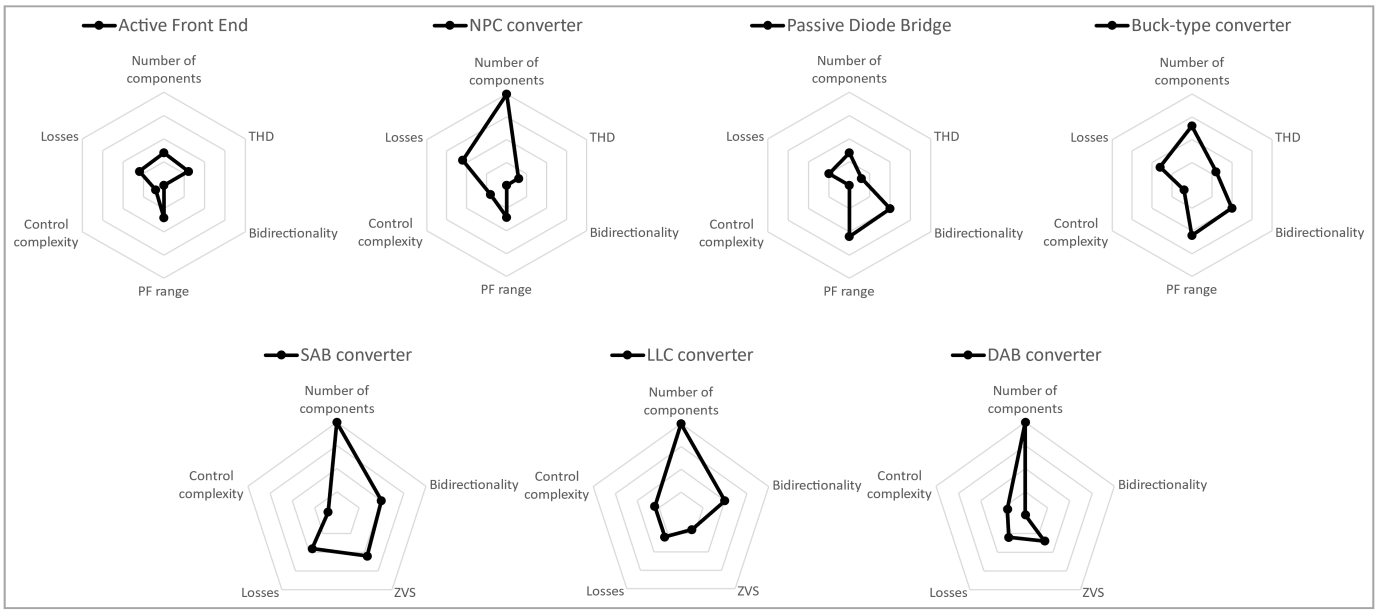

Fig. 10. Radar diagram of presented converters. The ac/dc converters have been compared by the number of components, THD, bidirectionality, power factor range, control complexity, and losses; the main reference of this comparison is [124]. The dc/dc converters have been compared by the number of components, bidirectionality, ZVS, losses, and control complexity; the main reference of this comparison is [125].

their use, especially when human exposure has the potential for injury. Product performance covers how well the product delivers its intended function in terms of efficiency, reliability, service life, and total cost of ownership.

In the mobility industry, the leading standards developing organizations (SDOs) are the Society of Automotive Engineers (SAE) in the U.S., the International Standards Organization (ISO), and the International Electrotechnical Commission (IEC) in Europe, Japan Aviation Electronics (JAE) and Japan–SAE (JSAE) in Japan, GB/T in China, and others.

A. General Aspects for Smart Grids

The U.S. Federal Energy Policy Act of 2005, under Section 1254, regulates the interconnecting of distributed resources with EPSs using the IEEE Standard [7].

The standards [126] and [127] describe the context of an SGAM at the component layer of domains (value creation chains) that comprise DER and distributed energy storage system (DESS) processes contrasted with hierarchical zones (automation pyramid) comprising field to market. Uslar et al. [128] expand this model into four additional, and overlaid, interoperability layers comprising communications

Authorized licensed use limited to: Universita degli Studi di Napoli Federico II. Downloaded on January 09,2025 at 10:42:23 UTC from IEEE Xplore. Restrictions apply.

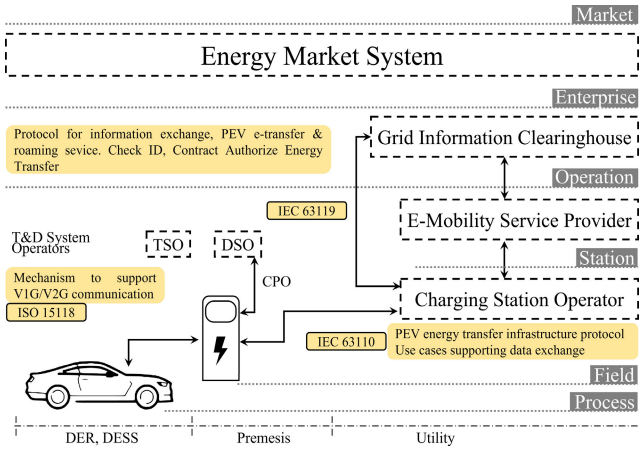

Fig. 11. SGAM with EVSE.

protocols, an information layer of data exchange models, and a function layer of functions and use cases, ending in a business layer of objectives and regulatory measures.

Fig. 11 illustrates this complex system of systems paradigm that defines the interoperability of DERs with the EPS, with the challenge being primarily one of standardization (or lack of). For example, [126] provides a protocol for PEV battery charging or discharging communications protocol at the site, [127] provides a protocol to manage PEV energy transfer infrastructure for charging station management, and [129] provides a protocol for roaming, authorization, and service access. However, in a larger context, a host of standards is necessary to address as many gaps in interoperability as possible be it environmental, process, protocol, use case, data exchange, communication mode, or cybersecurity, along with identification of gaps where new standards are needed.

The question arises as to how the processes, architectural zones, and interoperability layers, identified in Fig. 11, are utilized in the case of a UFCS. At the PEV to EVSE interface shown in Fig. 11, [130] standard defines the initialization and active engagement phases of energy transfer. These are parameters [18] such as EVSE max/min voltage and maximum injected or absorbed real or reactive power. The PEV evaluates and sends configuration information to the EVSE, again [18] parameters including power at overexcited and underexcited PF, vehicle manufacturer, inverter system model number, and input voltage. The initialization session concludes with the EVSE sending management information to the PEV ([18] management info) that includes [32] functions.

During initialization and active engagement phases, the smart SGIC, the EMSP, and the CPO shown in Fig. 11 are involved. The SGIC is a web portal for public access to a clearinghouse of information about the grids such as locations, standards, use cases, regulation, and policy, along with best practices and lessons learned. The EMSP is a company offering PEV charging service to customers and provides customers with facilities to identify locations of charging stations, initiate charging (or discharging), and pay for services through a variety of methods. A CPO manages PEV charging networks that may belong to multiple owners, such as public parking and shopping malls. The CPO, on the other hand, installs and maintains the charge stations, while the EMSP handles customer relationships and manages to charge service agreements.

Once the PEV initializes to the EVSE and grid, the active engagement phase commences. The EVSE is now the sole DME according to [18] functions. The EVSE via links to CPO, EMSP, and SGIC provides the PEV with authorization to discharge or charge. The PEV for its part must check with the EVSE every second to ensure the permit service authorization is valid, otherwise discontinue service. Finally, the PEV must provide the DME with monitoring information per [18] that includes operational status, voltage, frequency, active and reactive power, and UTC time stamp.

B. General Aspects for UFCSs

The main targets for EV conductive charging systems are IEC 61851 [131] and SAE J3072 [130]. In particular, in IEC 61851, Section I provides general requirements on EVSE, Sections 23 and 24 provide requirements for Mode 4 charging on dc EVSE connected with the grid at 1000 V in ac $50-60$ Hz with rated current not exceeding 250 A, in accordance with [46], and with connection to the vehicle at no more than 1500 V in dc with nominal current not exceeding 400 A.

The preferred values of the rated operational dc voltages of Mode 4 are 480, 600, 750, and 1000 V. The preferential rated dc currents are 70, 80, 125, 200, 250, and 400 A. The standard does not prescribe any specific electrical topology for EVSE Mode 4, but it provides instructions regarding the design specifications, the checks necessary for safe operation, and other functional requirements. The necessary design specifications concern the following.

1) *Devices and Components Used:* Electric devices and components of EVSE shall comply with their relevant standards. The standards also assign some requirements regarding reliability, lifestyles, utilization category, inrush current, overvoltage category, insulation resistance, touch current, and IP degrees.
2) *Protective Device and Conductor:* In EVSE Mode 4, fault protection is based on electric separation. Emergency switching or disconnect equipment shall be used either to disconnect the supply network from EVSE or to disconnect the socket outlet or the cable assembly from the supply network. The protective earth conductor and the protective conductor are of sufficient rating in accordance with the requirements of [132] and [133]. If the EVSE presents more than one connecting point used simultaneously, and they are connected to a common input terminal of the EVSE, each point must have individual protection incorporated in the EVSE. The standard also defines the breaking capacity of the devices and how to carry out measurements of leakage current and contact current and the electromagnetic compatibility tests. The station with a plug for dc charging of the EVs must be equipped with a residual current device (RCD), and it can be equipped with an overcurrent protection device. The mass of the charging station in the dc of the EV must be at the same potential as the external protective conductor.

Authorized licensed use limited to: Universita degli Studi di Napoli Federico II. Downloaded on January 09,2025 at 10:42:23 UTC from IEEE Xplore. Restrictions apply.

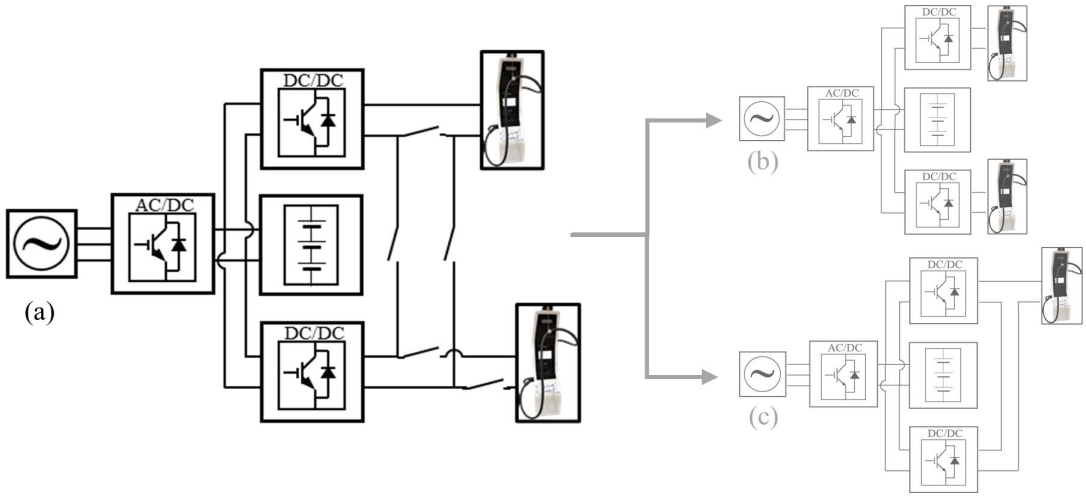

Fig. 12. Electric block scheme of the UFCS presented in [45] and [61]. Left: the overall structure may become the right one on the basis of the state of the switches. Right: the upper structure is able to charge two vehicles with a voltage of up to 450 V at the same time. The lower structure may charge one vehicle with a voltage of up to 900 V using the two dc–dc converters with the output connected in series.

3) *EVSE to EV Cable:* The voltage and current ratings of the cable assembly shall be compatible with the rating of the EVSE. A cable assembly must be a flexible tube, which may include one or more conduit cables or wires. The maximum cable length should be 5 m. The cable insulation is wear-resistant and maintains flexibility over the full temperature range required by the classification of the EVSE. Cables used with accessories, according to [134], for Mode 4, shall have a minimum withstand I^2t value of 80000 A^2s.
4) *Other Specification References:* Reference [135] standard regulates the safety requirements of power supplies, reactors, power transformers, and similar products. Reference [133] concerns the protection systems against electric shock; of interest for the EVSE are parts 4 and 5 that deal with the protection for low-voltage installations. Reference [136] relates to equipment within low-voltage systems and their insulation coordination systems. Reference [137] concerns low-voltage switchgear and control gear for their assembly reference shown in [132]. The standard applies to equipment that is designed to be used at an altitude of up to 2000 m. Reference [138] contains an overview of techniques to test low-voltage equipment under high-voltage supply, [139] prescribes the requirements for couplers for industrial purposes, socket outlets, and plugs, and [134] deals with plugs for conductive charging of EVs. Reference [140] regulates the safety requirements of electromechanical elementary relays. References [141] and [142], respectively, prescribe the safety of electronic and programmable boards and control and communication systems. Reference [143] regulates the safety in connection to an external electric power supply.

Reference [46] is the standard concerning the environmental tests to be carried out for the commissioning of electrotechnical systems. The standards of installation of the infrastructure, located in an open environment and open to the public, do not concern the design or electrical installation, so they are beyond the scope of this article.

The first step in researching EVSE requires identifying which configuration is compatible with the EV. Different configurations imply a different sequence of recharge enabling and a different implementation of the protection systems. The connection between the vehicle and the station must be made through cable and connector; therefore, the choice of the connector is the starting point of this analysis.

Reference [134] series specifies the requirements for plugs, fixed sockets, movable connectors, fixed connectors, and power cables described in [144]. Reference [134] deals with mechanical, electrical, and performance requirements for plugs, fixed sockets, mobile vehicle connectors, and fixed vehicle connectors to interface such dedicated charging equipment with the EV. Reference [131] divides connections into cases, types, and systems; this subdivision is not aimed to increase the complexity but to harmonize and group the different products existing before the formulation of the standard.

The MCS standard [145] is now under development and targets dc charging of HD vehicles up to 1500 V, 3000 A covering couplers, cables, communications, and interoperability for commercial applications. When completed, this standard will comprise the main document plus five dependents (slash J-docs) covering the listed subtopics. The goal is a higher reliability service at greater than 4-9's success rate for the first attempt.

C. Connection and Connectors

Indeed, based on whether the cable is connected or integral to the EVSE or with the EV, there are three cases [131].

Case A The cable is integrated into the vehicle, and it is connected to the supply network with a plug.

Case B Both vehicle and supply network have inlets to connect the plugs and cable.

Case C The cable is integrated into the dispenser and connected to the vehicle when required.

The overall usable length should not exceed a certain value unless equipped with a cable management system that is part of the listed EVSE. In the New York State Building Code [146], for example, this value is 7.5 m (25 ft).

Authorized licensed use limited to: Universita degli Studi di Napoli Federico II. Downloaded on January 09,2025 at 10:42:23 UTC from IEEE Xplore. Restrictions apply.

The standard [134]-3 extends the standard [134]-1 and describes the specific designs of connectors and sockets for charging EVs in dc in Mode 4.

1) *Config AA–CHAdeMO:* It implements System A according to [147] and uses CANbus communication according to [144] between the station and the vehicle; the nominal output voltage is limited to 600 V and 200 A in dc. It is based on the JEVS G105-1993 specifications, and it is mainly used in Japanese EVs.
2) *Config BB:* It implements System B according to [147] and uses a second CANbus communication [144] between the station and the vehicle, as reported in [134]-3; the nominal output voltage is limited to 750 V and 250 A in dc. It is based on the specifications of GB/T 20234.3, and it is mainly used in Chinese EVs.
3) *Config EE–CCS1:* It implements System C according to [147] and uses PLC communication according to [144] for higher level communication between the vehicle and the station. The nominal output voltage is limited to 600 V and 200 A in dc. It is based on the specifications of SAE J1772, and it is mainly used in the USA.
4) *Config FF–CCS2:* It implements System C and uses PLC communication. The nominal output voltage is limited to 1000 V and 200 A in dc. It is an evolved version of CCS1, and it is a global standard mainly used in the EU, the USA, and, India.

Although the Tesla Supercharger can only service Tesla vehicles, the latter can use adapters to convert CHAdeMO in Tesla protocol.

D. Communication

The communication between EVSE and EV works on the basic level and the high level [144].

1) *Base Communication:* It happens via the CP and manages the basic processes, such as charging start and normal/emergency stop.
2) *High-Level Communication:* This digital communication is implemented in different ways for different standard protocols. It works through the CAN bus on the CHAdeMO or through the CP circuit of PLC on the CCS.
3) *Human–Machine Interface:* Also, the user needs to interact with the charge. He/she must be able to start and stop the charge through an interface both on EVSE and EV.

The control of the EVSE must follow both static and dynamic regulation specifications [144].

1) *VCCF:* The EVs are equipped with onboard storage systems with different technologies, topologies, and electrical dimensions; therefore, the charging process must be completely managed by the BMS of the EV. The BMS of the EV manages and controls the charge through a VCCF. The EVSE must supply a voltage or a current to the EV on the basis of the request by the EV in the modalities of CVC or CCC. The maximum voltage limit can be changed during the charging process by the EV. In any case, the maximum nominal values are the minimum between those that can be supplied by the EVSE and those requested by the EV.
2) *CCC Mode:* The tolerance between the EVSE output current compared with the prescribed values sent by EV must be $\pm$ 2.5 A for prescriptions below 50 A and $\pm 5\%$ of the prescribed value for 50 A or more. The current must be adjusted by the EVSE to the value required by the EV, with a slew rate of at least 20 A/s for increasing current and 100 A/s for decreasing current in normal conditions. For the emergency stop and the fulfillment of general safety requirements, much higher reduction rates are required.

The ripple of the EVSE current in the CCC mode must not exceed the peak-to-peak values of 1.5 A at a frequency below 10 Hz, 6 A at a frequency below 5 kHz, and 9 A at a frequency below 150 kHz. The ripple of the current is not included in the tolerances defined for the gain and slew rate of the controlled system.

1) *CVC Mode:* The tolerance between the output voltages from the EVSE compared with the prescribed value sent by the EV must not be greater than 5% in the precharge phases and 2% in the CVC operation. The maximum voltage variation in normal operation must not exceed ± 20 V/ms and, in the case of load loss, must not exceed ± 250 V/ms. The maximum ripple of the voltage in normal operation must not exceed ± 5 V.
2) *Charge Rate Reporting:* Defined by SAE J2953/4 PEV charge rate reporting and test procedures.

E. Renewables and Storage Systems

In some topologies, the UFCSs integrate renewables and storage systems; the design and their positioning are subject to specific standards.

In [148], the design requirements for PV systems, such as electrical protection devices, dc array wiring, switching, and earthing provisions, are set out. In the analyzed system, the dc conditioning units include, but are not limited to, power conversion equipment, loads, or storage devices.

An advanced overview of the standardization of solar systems is to be found [149].

Reference [150] is an overview of the EES systems that are all electric systems able to store energy internally. The definitions of unit parameters, planning, test methods, installation, environmental, and safety issues are all provided. Reference [151] proposes a classification tool for primary batteries based on electrolytes, electrodes, system letters, and nominal values, as well as the maximum open-circuit voltage. Moreover, that paper deals with standardization with respect to nomenclature, dimensions, markings, terminal configurations, typical performance, test methods, and environmental and safety aspects.

Every country must follow the indications of the local fire-fighting department. The main request is to maintain a specific distance from dangerous/flammable materials. Although many customers are not worried about it, others prefer to avoid this kind of installation.

Authorized licensed use limited to: Universita degli Studi di Napoli Federico II. Downloaded on January 09,2025 at 10:42:23 UTC from IEEE Xplore. Restrictions apply.

F. Emerging New Trends

Many of the grid and PEV standards discussed are in the process of updating (every five years for SAE and others), a process that includes revision, reaffirmation, stabilization, or cancellation. In the area of high-power charging, the leading entities are CharIN and SAE. In 2018, the industry group CharIN focus group initiated a task force on MCS to consider as many industry viewpoints as possible regarding charging heavy-duty vehicles. The SAE J3271 MCS standard [145], currently under development, targets dc charging of HD vehicles up to 1500 V, 3000 A covering couplers, cables, communications, and interoperability for commercial applications. When completed, this standard will comprise the main document plus five dependents (slash J-docs) covering the listed subtopics. The goal is a higher reliability service at greater than 4-9's success rate for the first attempt.

Wireless charging is now standardized through [152] for light-duty vehicles. A persistent concern expressed for all such inductive power transfer technologies is an EMF, such as leakage or fringe fields in the vicinity of the inductive coupler [152]. More recently, high-power wireless energy transfer [a.k.a., wireless power transfer (WPT)] systems have been developed and are in commercial revenue service [153]. In this work, modular wireless charging pads communicate with similarly sized vehicle assembly receiver pads mounted beneath the vehicle chassis. When the electric transit bus operates along a municipal transit route receiving a charge at stops (opportunity charging), it is capable of an unlimited electric-only range.

High-power wireless charging systems initially had the same concern as EMF. Miller et al. [154] provide in-depth discussion, model, simulation, and experimental results of modular and scalable WPTs. Individual couplers are HD-LD interoperable up to 75 kW each with clusters capable of scaling throughput power in increments of 75 kW. The cited paper documents leakage fields at the perimeter of a transit bus in the area of the coupler at approximately 0.4 μT when the cumulative throughput power was at 265 kW. To put this into perspective, the ICNIRP 2010 guideline [155] for EMF is $<$27 μT, whereas the IEEE C95.1-2019 standard [156] for human exposure to EMF is $<$200 μT. The reason for such a dramatic EMF suppression has to do with the relative phasing of the individual couplers in relation to its adjacent coupler, with the most dramatic EMF reduction when operating in an antiphase.

V. Reliability and Safety Assessment

A. General Aspects

Reliability is defined as the ability of a system or a component to perform its intended function for an interval of time or at a specified moment. Terms such as repeatability, availability, and ability to maintain are often used in reliability assessment. A reliability assessment program for a product or a process is a knowledge-based and complex learning process, which plays a key role in the overall cost-effectiveness of systems.

The concept of reliability is often associated with that of safety even though both a working but not safe system and a safe but not working system can exist. A good practice in safety is to include the reliability constraints in the design phase of the system, so they become necessary conditions for a proper operation.

Each level of reliability assessment can be analyzed using different tools; the most solid and application-independent strategies are RBS, FMEA, and RCA.

B. Reliability Block Scheme

RBS is a technique to identify how the reliability of components impacts the reliability of the system under different operating conditions. The reliability function, $R(t)$, is defined as the probability of success of the system at time t. This probability is estimated through a detailed analysis (physics of failure), using reliability testing, or previous data sets and reliability modeling. The ''probability of failure" is represented as a symbolic equation, but it is difficult to predict its true value in practice.

In Fig. 13, an example of RBS is applied to the UFCS prototype in Fig. 12 and comprehensively reported in [45] and [61].

The multislot charging station in Fig. 12 is a dc microgrid [as in Fig. 5(b)] interfaced to the LV grid and equipped with BESS on the common dc bus [as in Fig. 4(d)]. The ac–dc converter is an AFE [as in Fig. 6(c)], the BESS is directly connected to the common dc bus, and there are SABs [as in Fig. 8(a)] converters between the dispensers of the two charging stations. The charger works in two different configurations.

1) The configuration in Fig. 12(b) is able to charge two vehicles with a voltage of up to 450 V at the same time.
2) A vehicle with a voltage up to 900 V can be charged using the two dc–dc converters with the outputs connected in series in the configuration shown in Fig. 11(c).

The maximum power provided by the grid is 50 kW; the BESS supplies the rest of the power to achieve 320 kW for two slots.

It is interesting to note that the RBS does not necessarily coincide with the physical block diagram. In Fig. 13, the subsystems appear to be in series or in parallel in different boxes of the table due to different operational conditions, even if the electric topology is usually the same.

This happens because charging one vehicle with a voltage range of 380 V needs the correct operation of one of the converters. However, charging one vehicle with a voltage range of 800 V requires both converters to work correctly. For this reason, there are different RBSs for the same system, thereby changing the reliability function.

Moreover, a potential result of this analysis is that charging two vehicles at the power range of 150 kW when the BESS is fully charged is less reliable than charging one vehicle with a voltage range of over 450 V at the power range of 150 kW, that is, $R_{1,5} < R_{2,2}$.

It is worth noting that the electrical system in Fig. 13 has more than one critical point. One dispenser is able to charge only one vehicle, and two dispensers are required to charge two vehicles at the same time. The BESS can supply the maximum power even without support from the grid; the grid cannot accommodate power for an ultrafast charge for even

Authorized licensed use limited to: Universita degli Studi di Napoli Federico II. Downloaded on January 09,2025 at 10:42:23 UTC from IEEE Xplore. Restrictions apply.

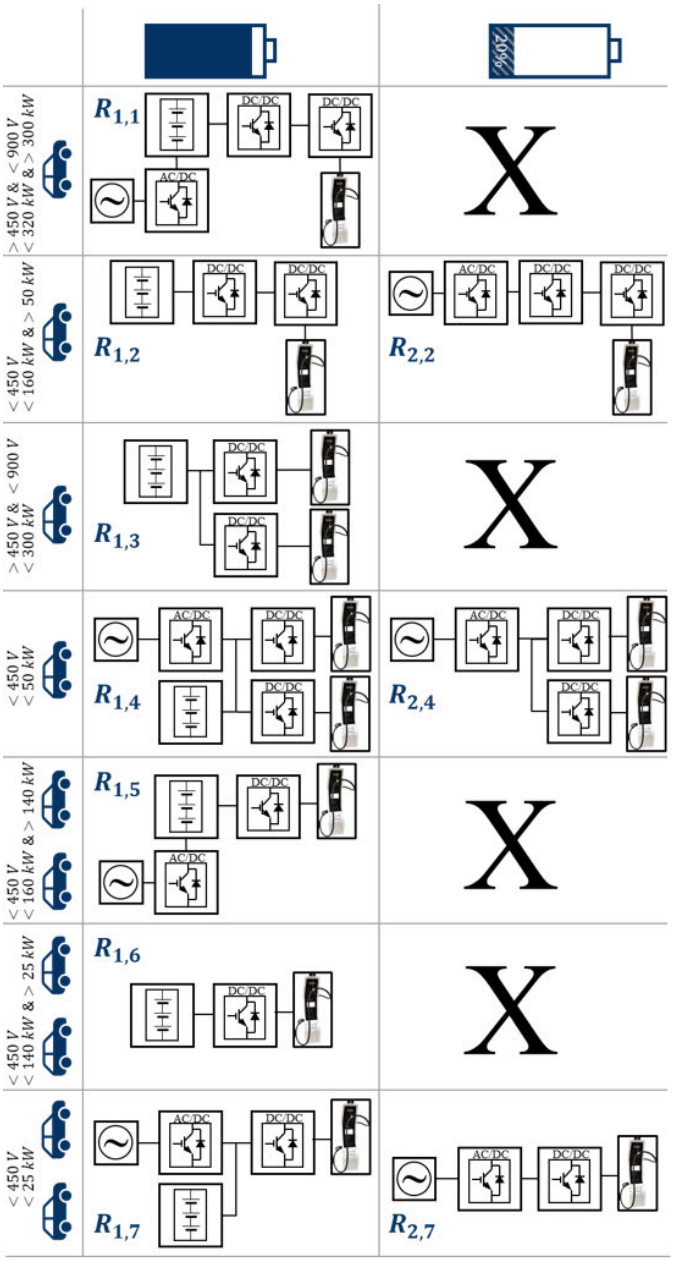

$$R_{1,1} = r_g \cdot r_{AC} \cdot r_b \cdot r_{DC1} \cdot r_{DC2} \cdot \left(1 - (1 - r_{d1})(1 - r_{d2})\right)$$
$$R_{1,2} = r_b \cdot r_{DC1} \cdot r_{DC2} \cdot \left(1 - (1 - r_{d1})(1 - r_{d2})\right)$$
$$R_{1,3} = r_b \cdot \left(1 - (1 - r_{DC1} \cdot r_{d1})(1 - r_{DC2} \cdot r_{d2})\right)$$
$$R_{1,4} = \left(1 - (1 - r_g \cdot r_{AC})(1 - r_b)\right)\left(1 - (1 - r_{DC1} \cdot r_{d1})(1 - r_{DC2} \cdot r_{d2})\right)$$
$$R_{1,5} = r_g \cdot r_{AC} \cdot r_b \cdot r_{DC1} \cdot r_{DC2} \cdot r_{d1} \cdot r_{d2}$$
$$R_{1,6} = r_b \cdot r_{DC1} \cdot r_{DC2} \cdot r_{d1} \cdot r_{d2}$$
$$R_{1,7} = \left(1 - (1 - r_g \cdot r_{AC})(1 - r_b)\right) \cdot r_{DC1} \cdot r_{DC2} \cdot r_{d1} \cdot r_{d2}$$
$$R_{2,2} = r_g \cdot r_{AC} \cdot r_{DC1} \cdot r_{DC2} \cdot \left(1 - (1 - r_{d1})(1 - r_{d2})\right)$$
$$R_{2,4} = r_g \cdot r_{AC} \cdot \left(1 - (1 - r_{DC1} \cdot r_{d1})(1 - r_{DC2} \cdot r_{d2})\right)$$
$$R_{2,7} = r_g \cdot r_{AC} \cdot r_{DC1} \cdot r_{DC2} \cdot r_{d1} \cdot r_{d2}$$

Fig. 13. RBS of the UFCS proposed in [45] and [61]. R_i is the reliability of the system in the different use cases, r_g refers to the grid, r_{AC} refers to the ac–dc converter, r_{DC1} and r_{DC2} refer to the two dc–dc converters, r_b refers to the battery, and r_{d1} and r_{d2} refer to the two dispensers.

one vehicle on its own. Both dc–dc converters must work to charge a vehicle with a voltage value of up to 900 V.

The structure in Fig. 13 could be improved by introducing redundancy, but this solution would drive up the price excessively. The best options are a good design and sizing of the subsystems, including the cooling system and the control system, to reduce the wear out of components and proper routine maintenance planning.

C. Reliability of Converters and Semiconductor Devices

Another method often used in studying the reliability of a system is to investigate the physical reliability of its components.

The faults of converters have various types that depend on the load, the dc-link voltage, and the control conditions of the converter. Sang et al. [157] analyze the short-circuit and open-circuit faults of the power switches in a distribution electronic power transformer (D-EPT). The current and voltage distortions in the output stage, input stage, and isolation stage are also evaluated.

Giannakis and Peftitsis [158] compare the performance and design requirements of four types of active rectifiers under a dc short-circuit condition. In [159], the impact of a short-circuit fault on the dc-link capacitor of an inverter/rectifier is discussed. In [160], the effects of an open-switch fault, due to problems with the switching devices, in a three-phase ac–dc PWM converter are analyzed. The result is that the unbalanced input ac currents, due to the faults, increase the harmonics and the ripple of the dc-link voltage. By considering the directions of a faulty phase current and the switching patterns of space vector PWM, the cause of the fault is determined. The authors propose a detection method and a fault-tolerant control method for open-switch faults to minimize the imbalance of the voltage ripple and input ac currents.

Power semiconductor devices are the most fragile components of power electronic systems; their reliability may depend on use, assembly, cooling, and environmental conditions. Stress factors, such as dust contamination, gas, current density, undervoltage and overvoltage, humidity, temperature, vibration, mechanical stress, pressure, radiation, and intensity of electrical and magnetic fields, also affect the device's reliability. The physical models use mostly the mean junction temperature and junction temperature fluctuations to represent the lifetime of power devices. The most common analytical models are the Norris–Landzberg model, the Coffin–Manson model, the Bayerer model, and the Lesit model [161].

The basis to improve the reliability of power electronic systems is the improvement of the reliability of power devices; therefore, many studies have focused on power device reliability in recent years. The state of the art in the reliability of power semiconductor devices is described in [161]. The analysis includes condition monitoring, failure mechanisms, active thermal control, and lifetime evaluation.

D. Reliability of Li-Ion BESS

The durability of Li-ion batteries is a timely topic of research. Many factors affect the Li-ion battery lifecycles, such as metallic lithium plating, collision and shock, formation of solid electrolyte interphase layer, vibration, deformation, and formation of lithium dendrite. One of the purposes of the BMS is to minimize or eliminate the consequences of Li-ion battery

Authorized licensed use limited to: Universita degli Studi di Napoli Federico II. Downloaded on January 09,2025 at 10:42:23 UTC from IEEE Xplore. Restrictions apply.

faults. Many faults diagnostic algorithms are proposed in the literature; they can be model-based or nonmodel-based.

The main faults in the Li-ion battery system are of two types [162].

1) *Internal Battery Faults:* Overdischarge, overcharge, external short circuit, internal short circuit, accelerated degradation, overheating, and thermal runaway. Model-based methods include structural analysis, state estimation, parameter estimation, and parity equation. The internal short-circuit faults are the main cause of EV safety, so they have become the focus in more recent works. Thermal fault detection is mainly conducted using battery thermal models.
   Nonmodel-based methods include knowledge-based methods and signal processing techniques. Even if they can improve the accuracy of fault diagnoses, they might require a large amount of data about fault conditions (often not available) or have very high computational costs, not suitable for the implementation on the BMS.
2) *External Battery Faults:* Cooling system fault, sensor fault, and cell connection fault. Model-based methods are those mainly implemented for external battery fault diagnosis; they help to detect cooling system faults and sensor faults. Among model-based methods, the entropy theory fault diagnosis and statistical analysis methods have been studied recently to analyze cell connection faults.

Predicting the useful lifetime of a battery is very complex because it strongly depends on the frequency of use and the charge and discharge curves. A BESS, as storage in a charging station, is subject seldom to a regular use, and its use is continuously influenced by the energy demand from the loads. When planning and sizing a charging station, estimating storage wear is crucial to predict maintenance costs (storage is typically the most expensive subsystem of the entire infrastructure).

One of the main strategies to increase the reliability of a subsystem is predictive maintenance. De Falco et al. [163] tried to predict the SoH of batteries using a multiple linear regression model based on historical data. The model operates with collected data of batteries under investigation and batteries characterized by accelerated degradation tests.

E. Safety Considerations

The safety requirements and equipment imposed by standards are the same for each conversion system installed outdoors. The devices already provided for the safety of users are switches, fuses, and isolation transformers; there are no further requests/requirements by standards.

A set of circuit breakers is required between the station and the charging station to protect the system in the case of overvoltage and for the grid when the system tries to supply energy to the grid in an incorrect manner due to a failure.

For outdoor installed systems equipped with storage with lithium batteries, the regulations imposed by the firefighters (potentially different for each area/country but in practice similar) always require a satellite topology of the station. The dispenser is the customer's only touch point, and the batteries are placed in a working area far from other flammable systems.

VI. Charging Data Usage

Smart charging via EMSP may allow the location owners, the vehicle owners, the CPO, and the DSO to trace the power and energy usage by EVs. In a smart charging station, the data including charging time, power, and so on for each vehicle are sent to a centralized cloud-based management platform.

This data may be visualized on a website, platform, or mobile application and analyzed in real time to make management of renewable sources activation, energy flows, and charging costs.

The massive data flows are subject to some cybersecurity vulnerabilities, caused by both the EVs and the charging infrastructures. Among the most common cybersecurity issues, some potential ones, pertaining to EVs, are listed in the following.

1) *Man-in-the-Middle:* The packet sniffer acts between the EV and the EVSE, thereby stealing monetary issues, tracking issues, and other privacy issues.
2) *Payment Fraud:* Tampering of the payment system.
3) *Malware on EV Control Unit:* The cyberattack on the vehicle via the EVSE can result in overcharging or discharging of batteries causing possible severe damage to batteries and taking the EV out of service.
4) *Denial-of-Service (DOS) Attack at EVSEs:* Taking charging station out of service (i.e., manipulation of emergency shut-down button).
5) Multiple compromised EVSEs can be used to increase the load by the grid causing grid failure.

The design of EVs and EVSEs must incorporate cybersecurity features from the beginning to reduce the risk of exploitation and product vulnerabilities. An interesting overview of how to incorporate cybersecurity in the design of an EVSE is presented in [164].

VII. Conclusion

This article provides an extended discussion on preliminary critical design considerations and choices to size a UFCS. The main contribution is pairing the requirements of both producers and customers with suitable solutions. Many comparisons and findings through benchmarking are presented to explore a wide range of solutions.

A matching table is presented to link the electrical converter's and microgrid's topologies with the boundary conditions of the distribution network (LV or MV) integrated with BESSs and/or RESs and the isolation requirements. The performance of converters is compared on the basis of many parameters: the number of components, THD, bidirectionality, power factor range, ZVS, control complexity, and losses.

An overview of the standards regarding the implementation and usage of UFCSs is obtained by investigating the existing norms related to the subject matter. The fundamentals of reliability and data usage are discussed since they are among the most critical topics in facility management and predictive maintenance.

Authorized licensed use limited to: Universita degli Studi di Napoli Federico II. Downloaded on January 09,2025 at 10:42:23 UTC from IEEE Xplore. Restrictions apply.

Finally, some promising solutions are suggested for both LV and MV distribution networks. In particular, in the MV distribution network, both ac and dc architecture can be implemented for UFCS. In the weak low-voltage distribution networks, the proposed UFC architecture is a dc microgrid with an integrated storage system in order to reduce the power impact of UFC on the grid. Other LV UFCs promising solutions concern not isolated dc/dc converters, such as PPP converters topologies, in order to improve conversion efficiency.

APPENDIX

An increasing number of carmakers are integrating UFC into their vehicles. The following list presents the latest examples.

2022 Ford Mustang Mach-E (SUV): It has a default battery pack of 70 kWh, with an optional extension of 91 kWh. The extended range pack can be charged in 45 min in the range between 10% and 80%.

2021 Volkswagen ID.4 (SUV): At a UFCS, it can charge from 5% to 80% in 38 min.

2022 Volvo C40 Recharge (SUV): It can be charged in the range between 10% and 80% in 35 min when using a charger with 150 kW of peak output.

2022 BMW i4 (Sedan): It can be charged in the range between 10% and 80% in 31 min and can take up to 200 kW.

2022 BMW iX (SUV): It can be charged in the range between 10% and 80% in 35 min and can take up to 200 kW. In 10 min, it can add 108 mi of range.

2022 Mercedes-Benz EQS (Sedan): With the ability to take up to 200 kW of charge, it can add 186 mi of range in 15 min.

2022 Rivian R1T (Pickup Truck): The maximum charging power is expected to start at 200 kW and be expanded to more than 300 kW in the future. Thus, in 20 min, it will be able to add 140 mi of range.

2021 Porsche Taycan (Sedan): It can charge from 5% to 80% in 22.5 min and can take up to 270 kW. It has $800-$ V architecture.

2022 Lucid Air Dream Edition (Sedan): It can take up to 300 kW. It has $900-$ V architecture.

2021 Tesla Model S (Sedan): It can add up to 200 mi in 15 min with a max charging power of 250 kW.

2022 Hyundai Ioniq 5 (SUV): It has a $77.4-$ kWh battery that can charge from 10% to 80% in less than 20 min when connected to 350 kW.

2022 Kia EV6 (SUV): It has a $77.4-$kWh battery that can charge from 10% to 80% in about 18 min when connected to 350 kW.

REFERENCES

[1] *Global EV Outlook 2021 Accelerating Ambitions Despite the Pandemic*, IEA, Paris, France, 2021.

[2] *Directive 2014/94/EU of the European Parliament and of the Council*, Eur. Parliament, Strasbourg, France, 2014, pp. 1–20.

[3] H. Engel, R. Hensley, S. Knupfer, and S. Sahdev, "Charging ahead: Electric-vehicle infrastructure demand," McKinsey Company, New York, NY, USA, Tech. Rep., 2018. [Online]. Available: https://www.mckinsey.com/industries/automotive-and-assembly/ourinsights/charging-ahead-electric-vehicle-infrastructure-demand

[4] P. Jochem, E. Szimba, and M. Reuter-Oppermann, "How many fast-charging stations do we need along European highways?" *Transp. Res. D, Transp. Environ.*, vol. 73, pp. 120–129, Aug. 2019.

[5] *European Union Infrastructure Electricity*, European Alternative Fuels Observatory EAFO, Moscow, Russia, 2018.

[6] D. Hall and N. Lutseyen, "Effects of battery manufacturing on electric vehicle life-cycle greenhouse gas emissions," ICCT, Berlin, Germany, Tech. Rep., 2018. [Online]. Available: https://theicct.org/publication/effects-of-battery-manufacturing-onelectric-vehicle-life-cycle-greenhouse-gas-emissions/

[7] *Smart Grids*, IEA, Paris, France, 2021.

[8] L. Hui-ling, B. Xiao-min, and T. Wen, "Impacts of plug-in hybrid electric vehicles charging on distribution grid and smart charging," in *Proc. IEEE Int. Conf. Power Syst. Technol. (POWERCON)*, Oct. 2012, pp. 1–5.

[9] J. Taylor, A. Maitra, M. Alexander, D. Brooks, and M. Duvall, "Evaluation of the impact of plug-in electric vehicle loading on distribution system operations," in *Proc. IEEE Power Energy Soc. Gen. Meeting*, Jul. 2009, pp. 1–6.

[10] S. J. Gunter, K. K. Afridi, and D. J. Perreault, "Optimal design of grid-interfaced EV chargers with integrated generation," in *Proc. IEEE PES Innov. Smart Grid Technol. (ISGT)*, Jan. 2012, pp. 1–8.

[11] S. J. Gunter, K. K. Afridi, and D. J. Perreault, "Optimal design of grid-connected PEV charging systems with integrated distributed resources," *IEEE Trans. Smart Grid*, vol. 4, no. 2, pp. 956–967, Jun. 2013.

[12] M. J. E. Alam, K. M. Muttaqi, and D. Sutanto, "A controllable local peak-shaving strategy for effective utilization of PEV battery capacity for distribution network support," *IEEE Trans. Ind. Appl.*, vol. 51, no. 3, pp. 2030–2037, May 2015.

[13] A. N. Brooks, "Vehicle-to-grid demonstration project: Grid regulation ancillary service with a battery electric vehicle," 2002.

[14] *SAE International*, document SAEJ2990, 2019.

[15] A. Dhabi, *Electricity Storage and Renewables: Costs and Markets to 2030*. Abu Dhabi, United Arab Emirates: IRENA, 2017.

[16] M. A. Hannan, M. M. Hoque, A. Mohamed, and A. Ayob, "Review of energy storage systems for electric vehicle applications: Issues and challenges," *Renew. Sustain. Energy Rev.*, vol. 69, pp. 771–789, Mar. 2017.

[17] K. C. Divya and J. Østergaard, "Battery energy storage technology for power systems—An overview," *Electr. Power Syst. Res.*, vol. 79, no. 4, pp. 511–520, Apr. 2009.

[18] *IEEE Standard for Interconnection and Interoperability of Distributed Energy Resources with Associated Electric Power Systems Interfaces*, Standard IEEE 1547-2018, 2018, pp. 1–138.

[19] A. Marinescu and I. Serban, "A smart residential microgrid based on renewable energy sources with integrated electric vehicle charging station," in *Proc. Int. Symp. Fundam. Electr. Eng. (ISFEE)*, Nov. 2018, pp. 1–5.

[20] H. Liu, Z. Hu, Y. Song, J. Wang, and X. Xie, "Vehicle-to-grid control for supplementary frequency regulation considering charging demands," *IEEE Trans. Power Syst.*, vol. 30, no. 6, pp. 3110–3119, Nov. 2015, doi: 10.1109/TPWRS.2014.2382979.

[21] N. Erdogan, F. Erden, and M. Kisacikoglu, "A fast and efficient coordinated vehicle-to-grid discharging control scheme for peak shaving in power distribution system," *J. Modern Power Syst. Clean Energy*, vol. 6, no. 3, pp. 555–566, May 2018.

[22] M. Singh, P. Kumar, and I. Kar, "Implementation of vehicle to grid infrastructure using fuzzy logic controller," *IEEE Trans. Smart Grid*, vol. 3, no. 1, pp. 565–577, Mar. 2012, doi: 10.1109/TSG.2011.2172697.

[23] M. Singh, P. Kumar, and I. Kar, "A model of electric vehicle charging station compatibles with vehicle to grid scenario," in *Proc. IEEE Int. Electr. Vehicle Conf.*, Mar. 2012, pp. 1–7

[24] B. Sah, P. Kumar, R. Rayudu, S. K. Bose, and K. P. Inala, "Impact of sampling in the operation of vehicle to grid and its mitigation," *IEEE Trans. Ind. Informat.*, vol. 15, no. 7, pp. 3923–3933, Jul. 2019, doi: 10.1109/TII.2018.2886633.

[25] Z. Wang and S. Wang, "Grid power peak shaving and valley filling using vehicle-to-grid systems," *IEEE Trans. Power Del.*, vol. 28, no. 3, pp. 1822–1829, Jul. 2013.

[26] A. Ouammi, "Peak loads shaving in a team of cooperating smart buildings powered solar PV-based microgrids," *IEEE Access*, vol. 9, pp. 24629–24636, 2021.

[27] J. Engels, B. Claessens, and G. Deconinck, "Optimal combination of frequency control and peak shaving with battery storage systems," *IEEE Trans. Smart Grid*, vol. 11, no. 4, pp. 3270–3279, Jul. 2020.

[28] Y. Guo, Q. Zhang, and Z. Wang, "Cooperative peak shaving and voltage regulation in unbalanced distribution feeders," *IEEE Trans. Power Syst.*, vol. 36, no. 6, pp. 5235–5244, Nov. 2021.

Authorized licensed use limited to: Universita degli Studi di Napoli Federico II. Downloaded on January 09,2025 at 10:42:23 UTC from IEEE Xplore. Restrictions apply.

[29] Y. Yu, O. S. Nduka, and B. C. Pal, "Smart control of an electric vehicle for ancillary service in DC microgrid," *IEEE Access*, vol. 8, pp. 197222–197235, 2020.

[30] T. T. Ku and C. S. Li, "Implementation of battery energy storage system for an island microgrid with high PV penetration," in *Proc. IEEE/IAS 56th Ind. Commercial Power Syst. Tech. Conf. (I&CPS)*, Jun. 2020, pp. 1–8.

[31] G. Bao, C. Lu, Z. Yuan, and Z. Lu, "Battery energy storage system load shifting control based on real time load forecast and dynamic programming," in *Proc. IEEE Int. Conf. Autom. Sci. Eng. (CASE)*, Aug. 2012, pp. 815–820.

[32] M. Bahadornejad, X. Gao, and N.-K.-C. Nair, "IEC 61850 based smart load-shifting through on-load tap changer control," in *Proc. IEEE PES Innov. Smart Grid Technol.*, Nov. 2011, pp. 1–7.

[33] J. Merrick, Y. Ye, and R. Entriken, "Assessing the system value of optimal load shifting," *IEEE Trans. Smart Grid*, vol. 9, no. 6, pp. 5943–5952, Nov. 2018.

[34] C. Li, X. Yu, W. Yu, G. Chen, and J. Wang, "Efficient computation for sparse load shifting in demand side management," *IEEE Trans. Smart Grid*, vol. 8, no. 1, pp. 250–261, Jan. 2017.

[35] C.-C. Lin, D.-J. Deng, W.-Y. Liu, and L. Chen, "Peak load shifting in the internet of energy with energy trading among end-users," *IEEE Access*, vol. 5, pp. 1967–1976, 2017.

[36] M. C. Vlot, J. D. Knigge, and J. G. Slootweg, "Economical regulation power through load shifting with smart energy appliances," *IEEE Trans. Smart Grid*, vol. 4, no. 3, pp. 1705–1712, Sep. 2013.

[37] Y. Wang, W. Saad, N. B. Mandayam, and H. V. Poor, "Load shifting in the smart grid: To participate or not?" *IEEE Trans. Smart Grid*, vol. 7, no. 6, pp. 2604–2614, Nov. 2016.

[38] B. Zhou, T. Littler, and A. Foley, "Electric vehicle capacity forecasting model with application to load levelling," in *Proc. IEEE Power Energy Soc. Gen. Meeting*, Jul. 2015, pp. 1–5.

[39] B. Zhou, D. Yang, S. Bu, G. Du, and T. Littler, "The impact of electric vehicle uncertainties on load levelling in the U.K.," in *Proc. IEEE Power Energy Soc. Gen. Meeting*, Jul. 2017, pp. 1–5.

[40] G. Shrinidhi, D. S. M, G. Rajesh, and S. Kochuvila, "Enhancement of electrical distribution system-load levelling," in *Proc. Int. Conf. Intell. Comput. Control Syst. (ICCS)*, May 2019, pp. 435–439.

[41] P. J. Ramirez, D. Papadaskalopoulos, and G. Strbac, "Co-optimization of generation expansion planning and electric vehicles flexibility," *IEEE Trans. Smart Grid*, vol. 7, no. 3, pp. 1609–1619, May 2016.

[42] P. Y. Kong and G. K. Karagiannidis, "Charging schemes for plug-in hybrid electric vehicles in smart grid: A survey," *IEEE Access*, vol. 4, pp. 6846–6875, 2016.

[43] J.-M. Clairand, J. Rodriguez-Garcia, and C. Alvarez-Bel, "Smart charging for electric vehicle aggregators considering users' preferences," *IEEE Access*, vol. 6, pp. 54624–54635, 2018.

[44] M. Dabbaghjamanesh, A. Kavousi-Fard, and J. Zhang, "Stochastic modeling and integration of plug-in hybrid electric vehicles in reconfigurable microgrids with deep learning-based forecasting," *IEEE Trans. Intell. Transp. Syst.*, vol. 22, no. 7, pp. 4394–4403, Jul. 2020.

[45] P. Franzese, D. Iannuzzi, F. Mottola, D. Proto, and M. Pagano, "Charging strategies for ultra-fast stations with multiple plug-in electric vehicle parking slots," in *Proc. AEIT Int. Annu. Conf. (AEIT)*, Sep. 2020, pp. 1–6.

[46] *International Electrotechnical Commission IEC Standard*, document IEC 60038, 2009.

[47] *Directive 2016/631/EU, European Parliament and of the Council*, European Parliament and the Council, Strasbourg, France, 2016.

[48] M. Vasiladiotis and A. Rufer, "A modular multiport power electronic transformer with integrated split battery energy storage for versatile ultrafast EV charging stations," *IEEE Trans. Ind. Electron.*, vol. 62, no. 5, pp. 3213–3222, May 2015.

[49] H. Iman-Eini, S. Farhangi, and J. L. Schanen, "A modular AC/DC rectifier based on cascaded H-bridge rectifier," in *Proc. 13th Int. Power Electron. Motion Control Conf.*, Sep. 2008, pp. 173–180.

[50] L. Camurca, X. Gao, L. F. Costa, and M. Liserre, "Design of a medium voltage DC fast charging station with grid voltage regulation and central modular multilevel converter," in *Proc. IEEE Energy Convers. Congr. Expo. (ECCE)*, Sep. 2018, pp. 2798–2804.

[51] D. Sha, G. Xu, and Y. Xu, "Utility direct interfaced charger/discharger employing unified voltage balance control for cascaded h-bridge units and decentralized control for CF-DAB modules," *IEEE Trans. Ind. Electron.*, vol. 64, no. 10, pp. 7831–7841, Oct. 2017.

[52] A. C. Nair and B. G. Fernandes, "A solid state transformer based fast charging station for all categories of electric vehicles," in *Proc. IECON 44th Annu. Conf. IEEE Ind. Electron. Soc.*, Oct. 2018, pp. 1989–1994.

[53] S. Sen, L. Zhang, T. Chen, J. Zhang, and A. Q. Huang, "Three-phase medium voltage DC fast charger based on single-stage soft-switching topology," in *Proc. IEEE Transp. Electrific. Conf. Expo. (ITEC)*, Jun. 2018, pp. 1123–1128.

[54] A. Q. Huang, Q. Zhu, L. Wang, and L. Zhang, "15 kV SiC MOSFET: An enabling technology for medium voltage solid state transformers," *CPSS Trans. Power Electron. Appl.*, vol. 2, no. 2, pp. 118–130, Jun. 2017.

[55] C. Zhu, "HighEfficiency, medium-voltage-input, solid-state-transformer-based 400-kW/1000-V/400-A extreme fast charger for electric vehicles," Office Energy Efficiency Renew. Energy Dept. Energy, Washington, DC, USA, Tech. Rep., Jun. 2019.

[56] X. She, X. Yu, F. Wang, and A. Q. Huang, "Design and demonstration of a 3.6kV-120 V/10KVA solid state transformer for smart grid application," in *Proc. IEEE Appl. Power Electron. Conf. Expo. (APEC)*, Mar. 2014, pp. 3429–3436.

[57] A. Moeini and S. Wang, "Design of fast charging technique for electrical vehicle charging stations with grid-tied cascaded H-bridge multilevel converters," in *Proc. IEEE Appl. Power Electron. Conf. Expo. (APEC)*, Mar. 2018, pp. 3583–3590.

[58] L. Gill, T. Ikari, T. Kai, B. Li, K. Ngo, and D. Dong, "Medium voltage dual active bridge using 3.3 kV SiC MOSFETs for EV charging application," in *Proc. IEEE Energy Convers. Congr. Expo. (ECCE)*, Sep. 2019, pp. 1237–1244.

[59] X. Liang, S. Srdic, J. Won, E. Aponte, K. Booth, and S. Lukic, "A 12.47 kV medium voltage input 350 kW EV fast charger using 10 kV SiC MOSFET," in *Proc. IEEE Appl. Power Electron. Conf. Expo. (APEC)*, Mar. 2019, pp. 581–587.

[60] M. M. Mahfouz and M. R. Iravani, "Grid-integration of battery-enabled DC fast charging station for electric vehicles," *IEEE Trans. Energy Convers.*, vol. 35, no. 1, pp. 375–385, Mar. 2020.

[61] D. Iannuzzi and P. Franzese, "Ultrafast charging station for electrical vehicles: Dynamic modelling, design and control strategy," *Math. Comput. Simul.*, vol. 184, pp. 225–243, Jun. 2021.

[62] P. Franzese, A. D. Pasquale, D. Iannuzzi, and M. Pagano, "Electric ultra fast charging stations: A real case study," in *Proc. AEIT Int. Annu. Conf. (AEIT)*, Oct. 2021, pp. 1–6.

[63] M. C. Falvo, D. Sbordone, I. S. Bayram, and M. Devetsikiotis, "EV charging stations and modes: International standards," in *Proc. Int. Symp. Power Electron., Electr. Drives, Autom. Motion*, Jun. 2014, pp. 1134–1139.

[64] M. C. Kisacikoglu, M. Kesler, and L. M. Tolbert, "Single-phase on-board bidirectional PEV charger for V2G reactive power operation," *IEEE Trans. Smart Grid*, vol. 6, no. 2, pp. 767–775, Mar. 2015, doi: 10.1109/TSG.2014.2360685.

[65] Z. Chen, N. Liu, X. Xiao, X. Yan, and Q. Liu, "Integrated mode and key issues of renewable energy sources and electric vehicles' charging and discharging facilities in microgrid," in *Proc. 2nd IET Renew. Power Gener. Conf. (RPG)*, 2013, pp. 2–22.

[66] M. A. Tabrizi, G. Radman, and A. Tamersi, "Micro grid voltage profile improvement using micro grid voltage controller," in *Proc. IEEE Southeastcon*, Mar. 2012, pp. 1–6.

[67] R. Wang, P. Wang, and G. Xiao, "Two-stage mechanism for massive electric vehicle charging involving renewable energy," *IEEE Trans. Veh. Technol.*, vol. 65, no. 6, pp. 4159–4171, Jun. 2016, doi: 10.1109/TVT.2016.2523256.

[68] D. Semenov, G. Mirzaeva, C. D. Townsend, and G. C. Goodwin, "An AC microgrid architecture and control strategy to achieve stability with any type of load," in *Proc. IEEE Southern Power Electron. Conf. (SPEC)*, Dec. 2017, pp. 1–6.

[69] N. L. Díaz, A. C. Luna, J. C. Vasquez, and J. M. Guerrero, "Centralized control architecture for coordination of distributed renewable generation and energy storage in islanded AC microgrids," *IEEE Trans. Power Electron.*, vol. 32, no. 7, pp. 5202–5213, Jul. 2017, doi: 10.1109/TPEL.2016.2606653.

[70] G. R. C. Mouli, P. Bauer, and M. Zeman, "Comparison of system architecture and converter topology for a solar powered electric vehicle charging station," in *Proc. 9th Int. Conf. Power Electron. ECCE Asia (ICPE-ECCE Asia)*, Jun. 2015, pp. 1908–1915.

[71] F. Locment and M. Sechilariu, "Modeling and simulation of DC microgrids for electric vehicle charging stations," *Energies*, vol. 8, pp. 4335–4356, 2015, doi: 10.3390/en8054335.

[72] T. Dragièević, X. Lu, J. C. Vasquez, and J. M. Guerrero, "DC microgrids—Part I: A review of control strategies and stabilization techniques," *IEEE Trans. Power Electron.*, vol. 31, no. 7, pp. 4876–4891, Jul. 2016, doi: 10.1109/TPEL.2015.2478859.

Authorized licensed use limited to: Universita degli Studi di Napoli Federico II. Downloaded on January 09,2025 at 10:42:23 UTC from IEEE Xplore. Restrictions apply.

[73] J. M. Guerrero, J. C. Vasquez, and R. Teodorescu, "Hierarchical control of droop-controlled DC and AC microgrids—A general approach towards standardization," in *Proc. 35th Annu. Conf. IEEE Ind. Electron.*, Nov. 2009, pp. 4341–4346.

[74] S. M. Kandil, H. E. Z. Farag, M. F. Shaaban, and M. Z. El-Sharafy, "A combined resource allocation framework for PEVs charging stations, renewable energy resources and distributed energy storage systems," *Energy*, vol. 143, pp. 961–972, 2018, doi: 10.1016/j.energy.2017.11.005.

[75] J. Hu, Y. Shan, Y. Xu, and J. M. Guerrero, "A coordinated control of hybrid AC/DC microgrids with PV-wind-battery under variable generation and load conditions," *Int. J. Elect. Power Energy Syst.*, vol. 104, pp. 583–592, 2019, doi: 10.1016/j.ijepes.2018.07.037.

[76] M. S. Rahman, M. J. Hossain, F. H. M. Rafi, and J. Lu, "EV charging in a commercial hybrid AC/DC microgrid: Configuration, control and impact analysis," in *Proc. Australas. Universities Power Eng. Conf. (AUPEC)*, Sep. 2016, pp. 1–6.

[77] L. Jia, Y. Zhu, and Y. Wang, "Architecture design for new AC-DC hybrid micro-grid," in *Proc. IEEE 1st Int. Conf. DC Microgrids (ICDCM)*, Jun. 2015, pp. 113–118.

[78] D. R. Aryani, J.-S. Kim, and H. Song, "Interlink converter with linear quadratic regulator based current control for hybrid AC/DC microgrid," *Energies*, vol. 10, p. 1799, 2017, doi: 10.3390/en10111799.

[79] S. Amirkhan, M. Radmehr, M. Rezanejad, and S. Khormali, "A robust control technique for stable operation of a DC/AC hybrid microgrid under parameters and loads variations," *Int. J. Elect. Power Energy Syst.*, vol. 117, 2020, doi: 10.1016/j.ijepes.2019.105659.

[80] E. Unamuno and J. A. Barrena, "Hybrid AC/DC microgrids—Part I: Review and classification of topologies," *Renew. Sustain. Energy Rev.*, vol. 52, pp. 1251–1259, 2015, doi: 10.1016/j.rser.2015.07.194.

[81] W. Lu et al., "Design and application of microgrid operation control system based on IEC 61850," *J. Mod. Power Syst. Clean Energy*, vol. 2, pp. 256–263, 2014, doi: 10.1007/s40565-014-0074-y.

[82] P. J. Hart, T. M. Jahns, and R. H. Lasseter, "Performance characteristics of a hybrid CERTS microgrid electric vehicle charging station," in *Proc. IEEE Energy Convers. Congr. Expo. (ECCE)*, Sep. 2014, pp. 3309–3316.

[83] X. Liu, P. Wang, and P. C. Loh, "A hybrid AC/DC microgrid and its coordination control," *IEEE Trans. Smart Grid*, vol. 2, no. 2, pp. 278–286, Jun. 2011, doi: 10.1109/TSG.2011.2116162.

[84] R. Majumder, "A hybrid microgrid with DC connection at back to back converters," *IEEE Trans. Smart Grid*, vol. 5, no. 1, pp. 251–259, Jan. 2014.

[85] P. C. Loh, D. Li, Y. K. Chai, and F. Blaabjerg, "Autonomous operation of hybrid microgrid with ac and DC subgrids," *IEEE Trans. Power Electron.*, vol. 28, no. 5, pp. 2214–2223, May 2013.

[86] B. Singh, B. N. Singh, A. Chandra, K. Al-Haddad, A. Pandey, and D. P. Kothari, "A review of three-phase improved power quality AC-DC converters," *IEEE Trans. Ind. Electron.*, vol. 51, no. 3, pp. 641–660, Jun. 2004.

[87] J. W. Kolar and T. Friedli, "The essence of three-phase PFC rectifier systems—Part I," *IEEE Trans. Power Electron.*, vol. 28, no. 1, pp. 176–198, Jan. 2013.

[88] A. Mohammadpour, M. R. Zolghadri, and M. Ferdowsi, "Constant input power control of a three phase isolated buck+boost rectifier," in *Proc. Intelec*, Jun. 2010, pp. 1–6.

[89] M. Su, H. Wang, Y. Sun, J. Yang, W. Xiong, and Y. Liu, "AC/DC matrix converter with an optimized modulation strategy for V2G applications," *IEEE Trans. Power Electron.*, vol. 28, no. 12, pp. 5736–5745, Dec. 2013, doi: 10.1109/TPEL.2013.2250309.

[90] D. Aggeler, F. Canales, H. Z.-D. L. Parra, A. Coccia, N. Butcher, and O. Apeldoorn, "Ultra-fast DC-charge infrastructures for EV-mobility and future smart grids," in *Proc. IEEE PES Innov. Smart Grid Technol. Conf. Eur. (ISGT Eur.)*, Oct. 2010, pp. 1–8.

[91] L. Tarisciotti, P. Zanchetta, A. Watson, J. C. Clare, M. Degano, and S. Bifaretti, "Modulated model predictive control for a three-phase active rectifier," *IEEE Trans. Ind. Appl.*, vol. 51, no. 2, pp. 1610–1620, Mar./Apr. 2015, doi: 10.1109/TIA.2014.2339397.

[92] P. CortÉs, J. RodrÍguez, P. Antoniewicz, and M. Kazmierkowski, "Direct power control of an AFE using predictive control," *IEEE Trans. Power Electron.*, vol. 23, no. 5, pp. 2516–2523, Sep. 2008, doi: 10.1109/TPEL.2008.2002065.

[93] D. E. Quevedo, R. P. Aguilera, M. A. Perez, P. Cortes, and R. Lizana, "Model predictive control of an AFE rectifier with dynamic references," *IEEE Trans. Power Electron.*, vol. 27, no. 7, pp. 3128–3136, Jul. 2012, doi: 10.1109/TPEL.2011.2179672.

[94] X. Liu, D. Wang, and Z. Peng, "A simplified direct finite-control-set model predictive control for AFEs with DC-link voltage dynamic reference design," in *Proc. 35th Chin. Control Conf. (CCC)*, Jul. 2016, pp. 4294–4299.

[95] M. Mehreganfar, M. H. Saeedinia, S. A. Davari, C. Garcia, and J. Rodriguez, "Sensorless predictive control of AFE rectifier with robust adaptive inductance estimation," *IEEE Trans. Ind. Informat.*, vol. 15, no. 6, pp. 3420–3431, Jun. 2019, doi: 10.1109/TII.2018.2879060.

[96] Z. Zhang, H. Fang, F. Gao, J. Rodríguez, and R. Kennel, "Multiple-vector model predictive power control for grid-tied wind turbine system with enhanced steady-state control performance," *IEEE Trans. Ind. Electron.*, vol. 64, no. 8, pp. 6287–6298, Aug. 2017, doi: 10.1109/TIE.2017.2682000.

[97] W. Luo, S. Vazquez, J. Liu, F. Gordillo, L. G. Franquelo, and L. Wu, "Control system design of a three-phase active front end using a sliding-mode observer," *IEEE Trans. Syst., Man, Cybern., Syst.*, vol. 52, no. 2, pp. 739–748, Feb. 2022, doi: 10.1109/TSMC.2020.3005212.

[98] T. Kang, C. Kim, Y. Suh, H. Park, B. Kang, and D. Kim, "A design and control of bi-directional non-isolated DC-DC converter for rapid electric vehicle charging system," in *Proc. 27th Annu. IEEE Appl. Power Electron. Conf. Expo. (APEC)*, Feb. 2012, pp. 14–21.

[99] N. Celanovic and D. Boroyevich, "A comprehensive study of neutral-point voltage balancing problem in three-level neutral-point-clamped voltage source PWM inverters," *IEEE Trans. Power Electron.*, vol. 15, no. 2, pp. 242–249, Mar. 2000.

[100] S. Rivera, B. Wu, J. Wang, H. Athab, and S. Kouro, "Electric vehicle charging station using a neutral point clamped converter with bipolar DC bus and voltage balancing circuit," in *Proc. IECON 39th Annu. Conf. IEEE Ind. Electron. Soc.*, Nov. 2013, pp. 6219–6226.

[101] L. Yacoubi, K. Al-Haddad, L. A. Dessaint, and F. Fnaiech, "Linear and nonlinear control techniques for a three-phase three-level NPC boost rectifier," *IEEE Trans. Ind. Electron.*, vol. 53, no. 6, pp. 1908–1918, Dec. 2006, doi: 10.1109/TIE.2006.881990.

[102] X. Zhang, G. Tan, T. Xia, Q. Wang, and X. Wu, "Optimized switching finite control set model predictive control of NPC single-phase three-level rectifiers," *IEEE Trans. Power Electron.*, vol. 35, no. 10, pp. 10097–10108, Oct. 2020, doi: 10.1109/TPEL.2020.2978185.

[103] R. Portillo, S. Vazquez, J. I. Leon, M. M. Prats, and L. G. Franquelo, "Model based adaptive direct power control for three-level NPC converters," *IEEE Trans. Ind. Informat.*, vol. 9, no. 2, pp. 1148–1157, May 2013, doi: 10.1109/TII.2012.2209667.

[104] G. Waltrich, J. L. Duarte, and M. A. M. Hendrix, "Multiport converter for fast charging of electrical vehicle battery," *IEEE Trans. Ind. Appl.*, vol. 48, no. 6, pp. 2129–2139, Nov./Dec. 2012.

[105] E. I. Pool-Mazun, J. J. Sandoval, P. N. Enjeti, and I. J. Pitel, "An integrated solid-state transformer with high-frequency isolation for EV fast-charging applications," *IEEE J. Emerg. Sel. Topics Ind. Electron.*, vol. 1, no. 1, pp. 46–56, Jul. 2020.

[106] Y. Du, S. Lukic, B. Jacobson, and A. Huang, "Review of high power isolated bi-directional DC-DC converters for PHEV/EV DC charging infrastructure," in *Proc. IEEE Energy Convers. Congr. Expo.*, Sep. 2011, pp. 553–560.

[107] P. He and A. Khaligh, "Comprehensive analyses and comparison of 1 kw isolated DC-DC converters for bidirectional EV charging systems," *IEEE Trans. Transport. Electrific.*, vol. 3, no. 1, pp. 147–156, Mar. 2017.

[108] B. Yang, F. C. Lee, A. J. Zhang, and G. Huang, "LLC resonant converter for front end DC/DC conversion," in *Proc. 17th Annu. IEEE Appl. Power Electron. Conf. Expo. (APEC)*, vol. 2, Mar. 2002, pp. 1108–1112.

[109] H. Wang, S. Dusmez, and A. Khaligh, "Maximum efficiency point tracking technique for LLC-based PEV chargers through variable DC link control," *IEEE Trans. Ind. Electron.*, vol. 61, no. 11, pp. 6041–6049, Nov. 2014.

[110] T. G. Grigorova and A. Stoyanov Vuchev, "Output and control characteristics of an LLC DC-DC converter operating above resonant frequency based on state plane analysis," in *Proc. 12th Nat. Conf. With Int. Participation (ELECTRONICA)*, May 2021, pp. 1–4.

[111] U. Kundu, S. Chakraborty, and P. Sensarma, "Automatic resonant frequency tracking in parallel LLC boost DC–DC converter," *IEEE Trans. Power Electron.*, vol. 30, no. 7, pp. 3925–3933, Jul. 2015, doi: 10.1109/TPEL.2014.2344021.

Authorized licensed use limited to: Universita degli Studi di Napoli Federico II. Downloaded on January 09,2025 at 10:42:23 UTC from IEEE Xplore. Restrictions apply.

[112] H. Akagi, T. Yamagishi, N. M. L. Tan, S.-I. Kinouchi, Y. Miyazaki, and M. Koyama, "Power-loss breakdown of a 750-V, 100-kW, 20-kHz bidirectional isolated DC-DC converter using SiC-MOSFET/SBD dual modules," in *Proc. Int. Power Electron. Conf. (IPEC-Hiroshima ECCE ASIA)*, May 2014, pp. 750–757.

[113] A. Kumar, A. H. Bhat, and P. Agarwal, "Comparative analysis of dual active bridge isolated DC to DC converter with double phase shift and triple phase shift control techniques," in *Proc. Recent Develop. Control, Autom. Power Eng. (RDCAPE)*, Oct. 2017, pp. 453–458.

[114] B. M. Kumar, A. Kumar, A. H. Bhat, and P. Agarwal, "Comparative study of dual active bridge isolated DC to DC converter with single phase shift and dual phase shift control techniques," in *Proc. Recent Develop. Control, Autom. Power Eng. (RDCAPE)*, Oct. 2017, pp. 453–458.

[115] S. Chi, P. Liu, X. Li, M. Xu, and S. Li, "A novel dual phase shift modulation for dual-active- bridge converter," in *Proc. IEEE Energy Convers. Congr. Expo. (ECCE)*, Sep. 2019, pp. 1556–1561.

[116] K. Shi, D. Zhang, Z. Zhou, M. Zhang, D. Zhang, and Y. Gu, "A novel phase-shift dual full-bridge converter with full soft-switching range and wide conversion range," *IEEE Trans. Power Electron.*, vol. 31, no. 11, pp. 7747–7760, Nov. 2016, doi: 10.1109/TPEL.2015.2512848.

[117] S. Bal, D. B. Yelaverthi, A. K. Rathore, and D. Srinivasan, "Improved modulation strategy using dual phase shift modulation for active commutated current-fed dual active bridge," *IEEE Trans. Power Electron.*, vol. 33, no. 9, pp. 7359–7375, Sep. 2018, doi: 10.1109/TPEL.2017.2764917.

[118] S. S. Shah and S. Bhattacharya, "A simple unified model for generic operation of dual active bridge converter," *IEEE Trans. Ind. Electron.*, vol. 66, no. 5, pp. 3486–3495, May 2019, doi: 10.1109/TIE.2018.2850012.

[119] X. Li and Y.-F. Li, "An optimized phase-shift modulation for fast transient response in a dual-active-bridge converter," *IEEE Trans. Power Electron.*, vol. 29, no. 6, pp. 2661–2665, Jun. 2014, doi: 10.1109/TPEL.2013.2294714.

[120] O. Garcia, P. Zumel, A. de Castro, and J. A. Cobos, "Automotive DC-DC bidirectional converter made with many interleaved buck stages," *IEEE Trans. Power Electron.*, vol. 21, no. 3, pp. 578–586, May 2006.

[121] D. Christen, S. Tschannen, and J. Biela, "Highly efficient and compact DC-DC converter for ultra-fast charging of electric vehicles," in *Proc. 15th Int. Power Electron. Motion Control Conf. (EPE/PEMC)*, Sep. 2012, pp. 1–9.

[122] J. Anzola et al., "Review of architectures based on partial power processing for DC-DC applications," *IEEE Access*, vol. 8, pp. 103405–103418, 2020.

[123] B. Jonathan, "International electrotechnical commission, brill | nijhoff," Brill, Tech. Rep., 2010, pp. 573–584, doi: 10.1163/ej.9789004163300.i-1081.494.

[124] H. Tu, H. Feng, S. Srdic, and S. Lukic, "Extreme fast charging of electric vehicles: A technology overview," *IEEE Trans. Transport. Electrific.*, vol. 5, no. 4, pp. 861–878, Dec. 2019.

[125] M. U. CUMA and M. M. SAVRUN, "Performance benchmarking of active-front-end rectifier topologies used in high-power, high-voltage onboard EV chargers," *Çukurova Üniversitesi Mühendislik Fakültesi Dergisi*, vol. 36, no. 4, pp. 1041–1050, 2021.

[126] *International Organization for Standardization*, document ISO/IEC 15118-1, 2019.

[127] *International Electrotechnical Commission IEC Standard*, document IEC 63110-1, 2022.

[128] M. Uslar et al., "Applying the smart grid architecture model for designing and validating system-of-systems in the power and energy domain: A European perspective," *Energies*, vol. 12, no. 2, p. 258, Jan. 2019.

[129] *International Electrotechnical Commission*, document IEC 63119-1, 2019.

[130] *Interconnection Requirements for Onboard, Utility-Interactive Inverter Systems*, document SAEJ3072, 2015, SAE International, 2015.

[131] *International Electrotechnical Commission IEC Standard*, document IEC 61851-1, 2017.

[132] *International Electrotechnical Commission IEC Standard*, document IEC 61439, 2020.

[133] *International Electrotechnical Commission IEC Standard*, document IEC 60364, 2017.

[134] *International Electrotechnical Commission IEC Standard*, document IEC 62196, 2015.

[135] *International Electrotechnical Commission IEC Standard*, document IEC 61558, 2017.

[136] *International Electrotechnical Commission IEC Standard*, document IEC 60664, 2020.

[137] *International Electrotechnical Commission IEC Standard*, document IEC 60947, 2021.

[138] *International Electrotechnical Commission IEC Standard*, document IEC 61180, 2016.

[139] *International Electrotechnical Commission IEC Standard*, document IEC 60309, 2021.

[140] *International Electrotechnical Commission IEC Standard*, document IEC 61810, 2015.

[141] *International Electrotechnical Commission IEC Standard*, document IEC 61508, 2010.

[142] *International Electrotechnical Commission IEC Standard*, document IEC 60950, 2004.

[143] *International Organization for Standardization ISO Standard*, document ISO 17409, 2020.

[144] *International Electrotechnical Commission IEC Standard*, document I1EC 61851-24, 2015.

[145] *SAE International*, document SAEJ3271, 2021.

[146] N. E. Code, *625.17 Cords and Cables*. New York, NY, USA: National Fire Protection Association (NFPA), 2020.

[147] *International Electrotechnical Commission IEC Standard*, document IEC 61851-23, 2015.

[148] *International Electrotechnical Commission IEC Standard*, document IEC 62548, 2016.

[149] J. H. Wohlgemuth, "Standards for PV modules and components—Recent developments and challenges," in *Proc. 27th Eur. Photovoltaic Solar Energy Conf. Exhib.*, Frankfurt, Germany, 2012, pp. 1–7.

[150] *Electrical energy storage (EES) systems - Part 1: Vocabulary*, document IEC 62933, 2018.

[151] *International Electrotechnical Commission IEC Standard*, document IEC 60086-1, 2021.

[152] J. Schneider et al., "Validation of wireless power transfer up to 11kW based on SAE J2954 with bench and vehicle testing," SAE Tech. Paper 2019-01-0868, 2019, doi: 10.4271/2019-01-0868.

[153] A. Calabro, B. Cohen, A. Daga, J. Miller, and F. Mcmahon, "Performance of 200-kW inductive charging system for range extension of electric transit buses," in *Proc. IEEE Transp. Electrific. Conf. Expo. (ITEC)*, Jun. 2019, pp. 1–5.

[154] J. M. Miller, A. W. Daga, F. J. McMahon, P. C. Schrafel, B. Cohen, and A. W. Calabro, "A closely coupled and scalable high-power modular inductive charging system for vehicles," *IEEE J. Emerg. Sel. Topics Power Electron.*, vol. 10, no. 3, pp. 3259–3272, Jun. 2022, doi: 10.1109/JESTPE.2020.3046382.

[155] A. Ahlbom et al., "Guidelines for limiting exposure to time-varying electric, magnetic, and electromagnetic fields (up to 300 GHz)," *Health Phys.*, vol. 74, no. 4, pp. 494–521, 1998.

[156] W. H. Bailey et al., "Synopsis of IEEE std C95.1–2019, 'IEEE standard for safety levels with respect to human exposure to electric, magnetic, and electromagnetic fields, 0 Hz to 300 GHz,"' *IEEE Access*, vol. 7, pp. 171346–171356, 2019.

[157] Z. Sang, C. Mao, J. Lu, and D. Wang, "Analysis and simulation of fault characteristics of power switch failures in distribution electronic power transformers," *Energies*, vol. 6, no. 8, pp. 4246–4268, Aug. 2013.

[158] A. Giannakis and D. Peftitsis, "Design considerations of power semiconductor devices employed in VSCs under short-circuit fault conditions in MVDC distribution grids," in *Proc. 20th Eur. Conf. Power Electron. Appl. (EPE ECCE Europe)*, Riga, Latvia, 2018, pp. P.1–P.11.

[159] A. M. Khelif, A. Bendiabdellah, and B. D. E. Cherif, "Short-circuit fault diagnosis of the DC-link capacitor and its impact on an electrical drive system," *Int. J. Electr. Comput. Eng. (IJECE)*, vol. 10, no. 3, p. 2807, Jun. 2020.

[160] W. S. Im, J. M. Kim, D. C. Lee, and K. B. Lee, "Diagnosis and fault-tolerant control of three-phase AC-DC PWM converter systems," *IEEE Trans. Ind. Appl.*, vol. 49, no. 4, pp. 1539–1547, Jul./Aug. 2013.

[161] B. Wang, "Review of power semiconductor device reliability for power converters," *CPSS Trans. Power Electron. Appl.*, vol. 2, no. 2, pp. 101–117, Jun. 2017.

[162] M.-K. Tran and M. Fowler, "A review of lithium-ion battery fault diagnostic algorithms: Current progress and future challenges," *Algorithms*, vol. 13, no. 3, p. 62, 2020.

[163] P. De Falco, L. P. Di Noia, and R. Rizzo, "State of health prediction of lithium-ion batteries using accelerated degradation test data," in *Proc. IEEE Texas Power Energy Conf. (TPEC)*, Feb. 2020, pp. 1–6.

[164] *DOE/DHS/DOT Volpe Technical Meeting on Electric Vehicle and Charging Station Cybersecurity Report*, document DOT-VNTSC-DOE-18-01, Mar. 2018. [Online]. Available: https://rosap.ntl.bts.gov/view/dot/34991

Authorized licensed use limited to: Universita degli Studi di Napoli Federico II. Downloaded on January 09,2025 at 10:42:23 UTC from IEEE Xplore. Restrictions apply.